이학석사학위논문

Epidemic dynamics and endemic states in scale-free uniform hypergraphs

척도 없는 균일 하이퍼그래프에서의 전염현상

2019년 8월

서울대학교 대학원
물리·천문학부
전 부 경

Epidemic dynamics and endemic states in scale-free uniform hypergraphs

척도 없는 균일 하이퍼그래프에서의 전염현상

지도교수 강 병 남

이 논문을 이학석사 학위논문으로 제출함

2019년 8월

서울대학교 대학원

물리·천문학부

전 부 경

전부경의 이학석사 학위논문을 인준함

2019년 8월

위 원 장 _____ (인)

부위원장 _____ (인)

위 원 _____ (인)

Abstract

Epidemic dynamics and endemic states in scale-free uniform hypergraphs

Bukyoung Jhun
Department of Physics and Astronomy
The Graduate School
Seoul National University

Hypergraph offers a framework to study the structure of more complicated, high-order interactions between agents. Recently, simplicial contagion process has been proposed as a complex contagion process in hypergraph. An SIS model whose infection spreads via simplicial contagion process is called a simplicial SIS model. We studied the simplicial SIS model in scale-free uniform hypergraphs. We applied the heterogeneous mean-field theory to study the properties of the phase transition in the model and performed numerical simulations in annealed hypergraphs to corroborate the mean-field theoretical predictions. The model showed various types of phase transition in the region where the exponent of the degree distribution is between two and three. The properties of the phase transition completely change according to the degree exponent. When the exponent is smaller than the critical degree exponent, the epidemic threshold vanishes and the susceptibility converges to a finite value in the vicinity of the phase transition. When the exponent is exactly the critical value, the model undergoes a second-order phase transition at a finite epidemic threshold, and

the susceptibility converges to a finite value in the vicinity of the phase transition. When the exponent is larger than the critical value, the model experiences a first-order phase transition at a finite epidemic threshold, and the susceptibility diverges in the vicinity of the phase transition. The critical value of the degree exponent depends on the size of the hyperedges d in the hypergraph and is between two and three. The numerical simulations in annealed scale-free 3- and 4-uniform hypergraphs corroborated the results.

Keywords : Epidemic process, SIS model, Scale-free network, Uniform hypergraph, Scale-free hypergraph, Phase transition

Student Number : 2017-24896

Contents

List of figures

Chapter 1

Introduction

Complex network has been used to understand systems whose interactions have heterogeneous and complicated structure. Before that, the main focus of physics had been lattice-like structures, where lattice points have identical or almost identical number of links connected to them. However, agents in many systems in the real-world are involved in heterogeneous number of interactions. The distribution of the number of interactions that an agent in the system is subject to often shows a power-law behavior [1–5]. In complex network, the number of links connected to a node (degree) is heterogeneous and can follow a power-law distribution. The degree distribution of a *scale-free network* has a power-law tail typically with the exponent between two and three.

Complex network has widely been used to describe variety of problems. It successfully enabled researchers to study the structure of the society [6, 7], spreading of epidemic diseases and innovations [8–11], opinion formation [12–14], and many other topics [15–19]. Contagion process through complex networks is an extensively studied topic. Many types of epidemic process, such as Susceptible-Infected-Susceptible (SIS) model [20–22], Susceptible-Infected-Recovered (SIR) model [23], and Susceptible-Weakened-Infected-Recovered (SWIR) model [24] have been studied in complex network. While the model was initially designed to study epidemic diseases, these models can describe social contagion phenomena. Extensive work has been devoted to the study of phase transitions and critical phenomena in the models [25–29].

A contagion process through a one-to-one contact in a network is called a *simple contagion* process. Many social phenomena that cannot be described by simple contagion process have been discovered [8, 30, 31]. In some cases, a contact with a single active neighbor is not enough to initiate change of the state an agent. A more sophisticated model of *complex contagion* process is required to understand such phenomena.

Simplicial contagion process has recently been proposed as a complex contagion process [32]. In the paper, the authors studied the proposed simplicial contagion process in simplicial complex, which is a type of hypergraph, but the process itself was defined for general hypergraph. *Hypergraph* is a generalization of network whose hyperedge connects two or more nodes in the hypergraph. Hypergraph has been used to study a variety of topics [33–40]. Simplicial contagion process is a more natural generalization than other complex contagion processes in hypergraph proposed before [41, 42], because it can be succinctly expressed in linear algebra by using adjacency tensor (see section 2.1).

We studied the susceptible-infected-susceptible model with simplicial contagion process, namely the simplicial SIS model, in uniform hypergraphs. A *uniform hypergraph* is a hypergraph all of whose hyperedges have the same size. If the size of hyperedges is d, it is called a d-uniform hypergraph or a d-hypergraph. Uniform hypergraphs can describe systems where a uniform number of agents interact at the same time. Also, hypergraphs that have hyperedges of almost the same size can be treated as a superposition of a small number of uniform hypergraphs.

In chapter 2, we present the *static model of uniform hypergraph*, a model of hypergraph in which we study the epidemic model. We will briefly present the definition of hypergraph and simplicial complex. Previously studied hypergraph ensembles

will be introduced. We will show that the degree distribution of the static model of uniform hypergraph has a power-law tail, hence it is scale-free.

In chapter 3, we present the heterogeneous mean-field theoretical study of simplicial SIS model. We will elaborate on the simplicial contagion process. We solved the self-consistency equation to obtain solutions for stationary states. We discovered that the properties of the phase transition, including the order of the phase transition completely change according to the exponent of the degree distribution. When the exponent of the degree distribution is between two and three, like many real-world systems, the simplicial SIS model showed rich phase transitions and critical phenomena, while the standard SIS model shows no phase transition in the region.

In chapter 4, we will present the results of numerical simulations in annealed scale-free 3- and 4-uniform hypergraphs. We will present the definition of annealed hypergraph, which is a mean-field theoretical treatment of a hypergraph ensemble. We used the quasistationary method, which is a computationally efficient method that had been proposed to study stationary states in non-equilibrium systems with absorbing states. The method will be elaborated in the chapter. We corroborated the mean-field theoretical predictions of the density of infection and the susceptibility.

Conclusions are drawn in chapter 5.

Chapter 2

Static model of d-uniform hypergraph

2.1 Hypergraph and simplicial complex

Hypergraph is a generalization of network that encodes group interactions between two or more agents. While an edge in a network contains (links) two nodes, a *hyperedge* in a hypergraph contains (links) two or more nodes. Formally, a hypergraph H is a pair $H = (X, E)$, where X is the set of nodes and E is a set of non-empty subsets of X: $E \subset \mathscr{P}(X) \backslash \{\emptyset\}$. An element of E is called a hyperedge. Hypergraph has been used to study ferromagnetic spin system [34, 35], academic collaboration [37, 43], population stratification [38], cellular network [36], and tagging [33, 39, 40].

A hypergraph all of whose hyperedges have the same size is called a *uniform hypergraph*. If the size of the hyperedges is d, it is called a d-uniform hypergraph or a d-hypergraph. Hence, a 2-uniform hypergraph is a network. If two or more identical hyperedges can be in a hypergraph, the hypergraph is called a *weighted* hypergraph. If all the hyperedges must be distinct, the hypergraph is called an *unweighted* hypergraph. If not otherwise specified, hypergraphs in this thesis is unweighted.

A hypergraph can be mapped into a bipartite network: view hyperedges as auxiliary nodes and connect each of them to the actual nodes (nodes in the hypergraph, as opposed to auxiliary nodes) that they contain in the hypergraph. The resulting network is called an *incident graph*, and is a bipartite graph because there is no connection between auxiliary nodes and between actual nodes. The incident graph is

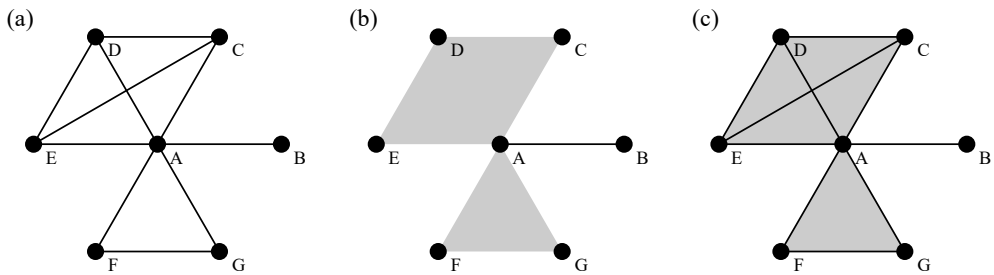

Fig. 2.1: (a) A Network, (b) a hypergraph, and (c) a simplicial complex representation of a collaboration structure: a 2-author paper is written by A and B, a four-author paper is written by A, C, D, and E, and a 3-author paper is written by A, F, G.

used to construct configuration model of hypergraph.

Abstract simplicial complex, or *simplicial complex* is a class of hypergraph with an extra constraint: if a hyperedge is in a simplicial complex, any non-empty subset of nodes in the hyperedge is also an hyperedge of the simplicial complex. This extra requirement makes simplicial complex an appropriate tool to study systems that the existence of a higher-order interactions (interactions that involves a large number of agents) implies the existence of lower-order interactions (interactions that involves a small number of agents) between any subset of the agents involved in the higher-order interaction. A hyperedge in a simplicial complex is often called a simplex. Simplicial complex has been used to study collaboration network [44, 45], semantic network [46], cellular network [47], and brain network [48, 49].

In simplicial complex, the generalized degree of a node is defined as the number of hyperedges of size d that contains the node [50, 51]. Adjacency tensor is also defined for each hyperedge sizes [52].

$$a_{\alpha}^{(d)} = \begin{cases} 1 & \text{if } \alpha \in S_d \\ 0 & \text{otherwise} \end{cases}, \tag{2.1}$$

where $|\alpha| = d$ and S_d is a set of hyperedges of size d in the simplicial complex. If a hyperedge in the simplicial complex is not a subset of any other hyperedge, the hyperedge is called a *facet*. List of facets in a simplicial complex determines the simplicial complex.

Extensive research has been devoted to simplicial complexes whose facets have one [52–54] or few [32] sizes. Therefore, research on uniform hypergraphs can benefit from the previous studies on simplicial complexes. For instance, a d-uniform hypergraph is uniquely expressed by a d-dimensional adjacency tensor. Canonical ensemble and microcanonical ensemble [52] of simplicial complexes can also be extended to uniform hypergraphs (see section 2.2 for detailed discussion). Other studies on simplicial complexes such as activity driven model [54] and centrality [47] can be applied to uniform hypergraphs.

2.2 Microcanonical and canonical ensemble of uniform hypergraph

Microcanonical and canonical ensemble of simplicial complex have recently been introduced [52]. They are unbiased ensembles with a given degree sequence and expected degree sequence, respectively. These ensembles can be applied to uniform and non-uniform hypergraphs.

Configuration model of uniform hypergraph and simplicial complex is a generalization of the configuration model of complex network. It has been defined in 3-uniform hypergraph [33], and in d-simplicial complexes [52]. It is an ensemble with a hard constraint of a fixed degree sequence. Therefore, it is the microcanonical ensemble of hypergraph, simplicial complex, and network. Configuration model of d-uniform hypergraph with a degree sequence $\{k_1, k_2, \cdots, k_N\}$ can be generated by

the following algorithm:

1. Prepare k_i stubs on each node $i = 1, 2, \cdots, N$. Additionally, place d stubs on each auxiliary node $\mu = 1, 2, \cdots, M$. Each auxiliary node represents a hyperedge. All stubs are initially unmatched. The total number of the auxiliary nodes is $M = \frac{1}{d}\sum_{i=1}^{N} k_i$.

2. Choose d stubs from the unmatched stubs of the actual nodes (nodes $i = 1, 2, \cdots, N$) with uniform probability.

3. If the chosen d stubs belong to d distinct nodes and no single auxiliary node is already connected to the chosen d nodes, connect the chosen nodes to an unmatched auxiliary node. Otherwise, perform step 2 again.

4. Repeat step 2–3 until all the stubs are matched or it is impossible to construct another hyperedge with the remaining nodes due to the constraints given in step 3. If the former is the case, we obtain the hypergraph. If the latter is the case, go to step 1.

Because self-loops and multiple identical hyperedges are forbidden, we might have to start over the algorithm from the beginning as illustrated in step 4. It is also possible that there is no unweighted hypergraph that has a given degree sequence. Whether a degree sequence corresponds to one or more hypergraphs can be identified by Erdős-Gallai theorem for $d = 2$ [55, 56], but not for $d \geq 3$. To bypass this difficulty, an efficient Markov chain Monte Carlo method to generate configuration model of d-dimensional simplicial complex or uniform hypergraphs has been developed [57].

Canonical ensemble of uniform hypergraph and d-dimensional simplicial complex is an unbiased ensemble with a given expected degree sequence. It maximizes

the entropy

$$S = -\sum_{G} P(G) \ln P(G) \tag{2.2}$$

under the constraint of a fixed expected degree sequence $\langle k_i \rangle$, $i = 1, 2, \cdots, N$. The summation runs over all possible uniform hypergraph G, or equivalently over all possible adjacency tensor a.

For large N, the probability that the hypergraph contains a hyperedge $\alpha = \{i_1, i_2, \cdots, i_d\}$ is

$$f_\alpha = d! \frac{\Pi_{r \in \alpha} \langle k_r \rangle}{(\langle k \rangle N)^d}. \tag{2.3}$$

The equation is valid for $f_\alpha \ll 1$. Canonical ensemble of d-uniform hypergraph can be constructed by adding $N \langle k \rangle / d$ hyperedges to the hypergraph with set nodes α chosen with probability f_α provided in Eq. 2.3.

2.3 Static model of hypergraphs

The *static model* of complex network [58, 59] has widely been used to study physics in scale-free networks due to its simple, intuitive definition and the computational efficiency to generate large scale networks. It has been used to study q-state Potts model [60], sandpile model [61], spin glass [62], and many other topics [63–66] in complex network.

The *static model of uniform hypergraph* is a generalization of the static model of complex network. The static model of d-uniform hypergraph is generated by the following algorithm:

1. Each of the N nodes is assigned a weight p_i, where p_i is given,

$$p_i = \frac{i^{-\mu}}{\zeta_N(\mu)} \simeq \frac{1-\mu}{N^{1-\mu}} i^{-\mu}, \tag{2.4}$$

where $\zeta_N(\mu) = \sum_{j=1}^{N} j^{-\mu}$. The normalization condition $\sum_{i=1}^{N} p_i = 1$ is satisfied.

2. Select d distinct nodes each with probability p_i. If the hypergraph does not contain any hyperedge consist of the chosen d nodes, add such hyperedge to the hypergraph.

3. Repeat step 2 for NK times.

Then, each node i has expected degree $\langle k_i \rangle$ The expected degree follows a power-law distribution $P(k) \sim k^{-\lambda}$. The minimum expected degree $\langle k_i \rangle_{\min} = \frac{N^{-\mu} N \langle k \rangle}{\sum_{n=1}^{N} j^{-\mu}}$ converges to a finite value $\frac{\lambda-2}{\lambda-1} \langle k \rangle$ and the maximum expected degree $\langle k_i \rangle_{\max} = \frac{N \langle k \rangle}{\sum_{n=1}^{N} j^{-\mu}} \to \frac{\lambda-2}{\lambda-1} \langle k \rangle N^{1/(\lambda-1)} \sim N^{1/(\lambda-1)}$ diverges.

2.3.1 Degree distribution

The probability that a node-i has a degree equal to k in a realization of the static model follows the Poisson distribution: $P_i^{(R)}(k) \simeq \langle k_i \rangle^k \exp(-\langle k_i \rangle)/k!$, because the node is selected to be in a new hyperedge in each loop of the construction algorithm by probability $1-(1-p_i)^d \simeq d p_i$. The degree distribution $P^{(R)}(k)$ is then,

$$P^{(R)}(k) = \frac{1}{N} \sum P_i(k) \simeq \int_{\langle k_i \rangle_{\min}}^{\langle k_i \rangle_{\max}} d\langle k_i \rangle P(\langle k_i \rangle) \frac{\langle k_i \rangle^k \exp(-\langle k_i \rangle)}{k!} \tag{2.5}$$

$$= \frac{(\lambda-1)}{\langle k_i \rangle_{\min}^{-\lambda+1} - \langle k_i \rangle_{\max}^{-\lambda+1}} \frac{1}{k!} \int_{\langle k_i \rangle_{\min}}^{\langle k_i \rangle_{\max}} d\langle k_i \rangle \langle k_i \rangle^{-\lambda+k} \exp(-\langle k_i \rangle). \tag{2.6}$$

For $N \to \infty$, $\langle k_i \rangle_{\max} \to \infty$ and $\langle k_i \rangle_{\min} \to \frac{\lambda-2}{\lambda-1} \langle k \rangle$. Therefore,

$$\lim_{N\to\infty} P^{(R)}(k) = (\lambda-1) \langle k_i \rangle_{\min}^{\lambda-1} \frac{\Gamma(-\lambda+k+1, \langle k_i \rangle_{\min})}{\Gamma(k+1)} \sim k^{-\lambda} \tag{2.7}$$

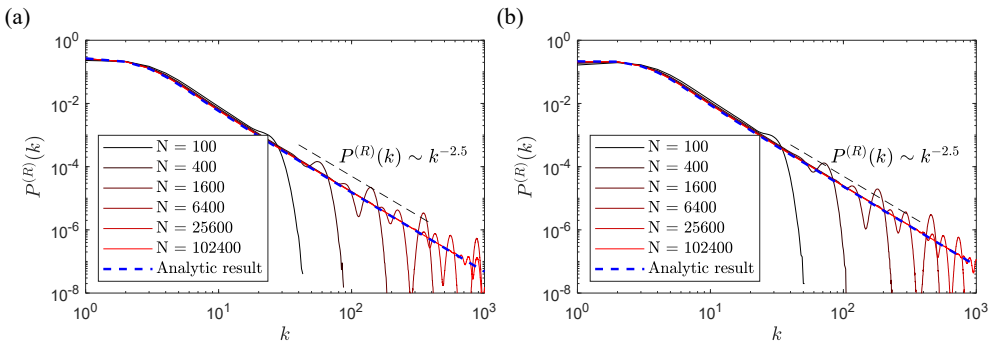

Fig. 2.2: The degree distribution of the static model of (a) 3-uniform and (b) 4-uniform hypergraph whose expected degree distribution has a power-law tail of exponent $\lambda = 2.5$. Redder lines denote larger system sizes. The dashed blue line is the analytic result expressed in Eq. 2.7. The number of nodes used in the simulation N is 100, 400, 1600, 6400, 25600, and 102400. As the system size is increased, the tail of the degree distribution extends and approaches the power-law distribution with the exponent $\lambda = 2.5$.

for sufficiently large k. Therefore, the tail of the degree distribution of the static model of uniform hypergraph follows the power-law with the exponent $\lambda = 1 + \frac{1}{\mu}$. The degree distributions obtained numerically for $d = 3$ and $d = 4$ with $\lambda = 2.5$ are illustrated in Fig. 2.2. The distribution has a power-law tail with the exponent $\lambda = 1 + \frac{1}{\mu} = 2.5$.

2.3.2 Probability of a hypergraph

The probability that a hyperedge $\{i_1 \cdots i_d\}$ is present in a static model of uniform hypergraph is

$$f_{i_1 \cdots i_d} = 1 - (1 - d! p_{i_1} \cdots p_{i_d})^{NK} \simeq 1 - e^{-d!NK p_{i_1} \cdots p_{i_d}}, \tag{2.8}$$

and the probability that a hypergraph G is generated is

$$P(G) = \prod_{\{i_1, \cdots, i_d\} \in G} \left(1 - e^{-d!NK p_{i_1} \cdots p_{i_d}}\right) \prod_{\{i_1, \cdots, i_d\} \notin G} e^{-d!NK p_{i_1} \cdots p_{i_d}}. \tag{2.9}$$

For any $\{i_1 \cdots i_d\}$ with a repeated index $i_n = i_m$, the probability $f_{i_1 \cdots i_d}$ is zero because of the prohibition of self-loops. Since $d!NKp_{i_1} \cdots p_{i_d} \sim N^{d\mu-d+1} / (i_1 \cdots i_d)^{\mu}$, when $0 < \mu < \frac{d-1}{d}$, which corresponds to $\lambda > 2 + \frac{1}{d-1}$,

$$f_{i_1 \cdots i_d} \simeq d!NKp_{i_1} \cdots p_{i_d}. \tag{2.10}$$

This is identical to the probability f_α of the canonical ensemble. However, in the case of $2 < \lambda < 2 + \frac{1}{d-1}$,

$$f_{i_1 \cdots i_d} \simeq \begin{cases} 1 & (i_1 \cdots i_d)^{\mu} \ll N^{d\mu-d+1} \\ d!NKp_{i_1} \cdots p_{i_d} & (i_1 \cdots i_d)^{\mu} \gg N^{d\mu-d+1} \end{cases}. \tag{2.11}$$

The fraction of nodes that satisfies the second case of Eq. 2.11 is proportional to $1 - AN^{d\mu-d}$ (where A is a constant) converges to 1 as $N \to \infty$. For $d = 2$, the static model of uniform hypergraph is identical to the static model of complex network. For $\mu = 0$ and equivalently $\lambda = \infty$, the expected degree of all node is identical and the model yields Erdős-Renyi-like hypergraphs.

Chapter 3

Mean-field theory of simplicial SIS-model in scale-free d-uniform hypergraph

3.1 Simplicial contagion process

A contagion process through a one-to-one interaction via an edge in a network is called a *simple contagion* process. Extensive work has been devoted to study simple contagion processes in complex network to describe disease spreading [67, 68], adoption of innovation [10, 69], and opinion formation [12–14]. However, social phenomena that cannot be reduced to a simple contagion process have been observed. For instance, the credibility of bizarre urban legend [70], the adoption of unproven new technologies [71], willingness to participate in risky migrations [72], the appeal of avantgarde fashion [73] depend on the contacts with multiple prior adoptors. Adoption of behaviors that are costly, risky, or controversial often requires an affirmation or reinforcement from an independent source.

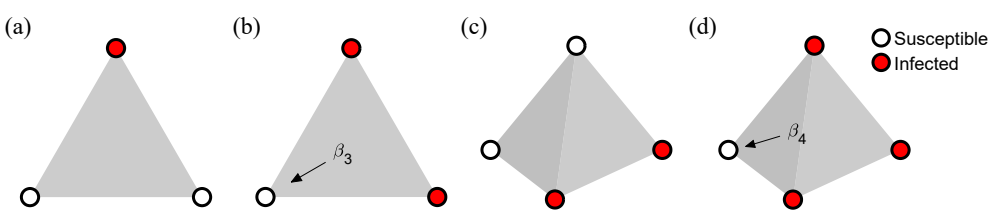

Fig. 3.3: Definition of simplicial contagion process through hyperedges of size (a, b) 3 and (c, d) 4. Only when $d-1$ nodes in a hyperedge of size d is infected, the infection spreads to the other one susceptible node through the hyperedge by rate β_d.

More complicated models of contagion, namely *complex contagion process*, have been proposed to describe social phenomena that cannot be characterized by simple contagion processes. The threshold model [74, 75], generalized epidemic model [24, 28], and bootstrap percolation [76] are some examples.

Recently, *simplicial contagion* process has been proposed as a complex contagion process in hypergraphs. The simplicial contagion process describes maximally conservative contagion process in hypergraphs. Contagion through a hyperedge of size d occurs only when all but one of the nodes in the hyperedge is infected. In such case, the one susceptible node is infected by a rate β_d per unit time. For instance, when the node j and k are infected, and the hyperedge $\{i, j, k\}$ is in the hypergraph, the node i is infected through the hyperedge by probability $\beta_3 dt$ in infinitesimal duration dt. If only the node j is infected and the node k is not, the infection does not spread to the node i through the hyperedge.

Simplicial SIS model is SIS model where the infection is spread via simplicial contagion process. Each node is in either susceptible (S) or infected (I) state. The recovery process (I $\rightarrow$ S) is defined the same as the SIS model of network because the recovery process takes place on each node independently, making it irrelevant of the structure of the contagion process. If a node is the infected (in I state), it is turned to the susceptible state (recovery) by rate μ. Susceptible nodes are turned to infected state by simplicial contagion process.

$$I \rightarrow S \tag{3.1}$$

$$(d-1)I + S \rightarrow dI. \tag{3.2}$$

Simplicial SIS model is originally defined to describe complex contagion pro-

cess in simplicial complexes, but as pointed out in the original paper, the process itself is defined for general hypergraphs. It can be especially useful in uniform hypergraphs, since the process is naturally described by an adjacency tensor of dimension d.

$$p_i' = (1-\mu dt)\, p_i + \frac{1}{(d-1)!}(1-p_i)\,\beta_d dt \sum_{i_2,\cdots,i_d} a_{i_1\cdots i_d} p_{i_2}\cdots p_{i_d} \tag{3.3}$$

$$\frac{d}{dt}p_i = -\mu p_i + \frac{1}{(d-1)!}(1-p_i)\,\beta_d \sum_{i_2,\cdots,i_d} a_{i_1\cdots i_d} p_{i_2}\cdots p_{i_d}. \tag{3.4}$$

For instance, when $d=2$ and $d=3$,

$$\frac{d}{dt}p_i = -\mu p_i + (1-p_i)\,\beta_2 \sum_j a_{ij} p_j \tag{3.5}$$

$$\frac{d}{dt}p_i = -\mu p_i + \frac{1}{2}(1-p_i)\,\beta_3 \sum_{j,k} a_{ijk} p_j p_k. \tag{3.6}$$

For 2-uniform hypergraphs, which are networks, the equation is identical to that of the simple one-to-one contagion process, making this definition a natural generalization of the epidemic process in complex networks to hypergraphs. For small p, we can ignore the higher order terms.

$$\frac{d}{dt}p_i = -\mu p_i + \frac{1}{d!}\beta_d \sum_{i_2,\cdots,i_{d+1}} a_{i_1\cdots i_{d+1}} p_{i_2}\cdots p_{i_{d+1}}. \tag{3.7}$$

Since $a_{i_1\cdots i_{d+1}}$ is a symmetric tensor, it can be diagonalized [77]. The equation then becomes,

$$a_{i_1\cdots i_{d+1}} = \sum_\ell \Lambda_\ell u_{\ell i_1} u_{\ell i_2}\cdots u_{\ell i_d} \tag{3.8}$$

$$p_i(t) = \sum_j c_j(t) u_{ji} \tag{3.9}$$

$$\sum_\ell \left[\frac{dc_\ell(t)}{dt} - \mu c_\ell(t) + \beta \Lambda_\ell c_\ell(t)^{d-1} \right] u_{\ell i} = 0 \tag{3.10}$$

$$\frac{dc_\ell(t)}{dt} - \mu c_\ell(t) + \beta \Lambda_\ell c_\ell(t)^{d-1} = 0. \tag{3.11}$$

Several definitions of complex contagion process in hypergraph have previously been suggested before simplicial contagion process [41, 42]. These contagion models, however, are not expressed concisely in linear algebra.

The simplicial contagion process can be understood as a threshold model in a hypergraph. In the threshold model of complex network, the contagion occurs when the number or the portion of infected neighbors exceeds a certain threshold. In the simplicial contagion model, contagion through a hyperedge occurs when the number of infected nodes in the hyperedge is larger than a threshold. Also, the threshold is one less than the size of the hyperedge, which makes this model a maximally conservative threshold model of hypergraphs.

In this chapter, we study the simplicial SIS model in scale-free uniform hypergraphs. We performed mean-field theoretical calculations on d-uniform hypergraph of arbitrary value of d and numerical simulations on 3- and 4-uniform hypergraphs. We discovered that in scale-free uniform hypergraphs with degree exponent between two and three exhibit various types of phase transitions. Note that in scale-free networks, the mean-field theory of SIS model predicted a vanishing epidemic threshold for $2 < \lambda \leq 3$ [20, 21]. Because the degree exponents of most of the real-world scale-free networks are between two and three, SIS model in such network does not show phase transition.

All hypergraphs, including networks, are combinations of uniform hypergraphs.

Therefore, we believe that epidemic processes in non-uniform hypergraphs can be understood by studying the processes in uniform hypergraphs and the effect of their superpositions.

3.2 Heterogeneous mean-field theoretical calculation

We applied the heterogeneous mean-field theory to study the stationary states of the system. The heterogeneous mean-field theoretical approach has been successfully used to study SIS [20, 21] and SIR [23] model in scale-free networks. It incorporates the significant effect of small portion of nodes that have large degrees. In heterogeneous mean-field theory, all nodes with the same degree are treated statistically equivalent. We established a differential equation for the infection probability of nodes with degree k, and then find the stationary solutions of the probability. Then we solve a self-consistency equation to calculate the density of infection and other properties of the system.

We found that the simplicial SIS model in scale-free uniform hypergraphs shows rich phase transition pattern. The properties of the phase transition completely change according to the exponent of the degree distribution λ. When λ is smaller than a critical value λ_c, which is determined by the size of hyperedges, there is always a non-trivial stationary state for arbitrarily small contagion rate. The critical value is given $\lambda_c = 2 + \frac{1}{d-1}$, hence it is between two and three. When the contagion rate approaches zero, so does the density of infection of the non-trivial stationary state. The susceptibility, which is proportional to the sensitivity to the rate of voluntary infection (see section 3.2.4 for the definition and detailed discussions.), approaches 1 as the contagion rate approaches zero. The order parameter critical exponent is larger than 1 and the susceptibility critical exponent is zero. When λ is exactly the critical

value, the system undergoes a second-order phase transition at finite contagion rate. This means that the epidemic threshold is discontinuous with respect to λ at the critical value. The susceptibility converges to a finite value in the vicinity of the phase transition. The order parameter critical exponent is larger than 1 and the susceptibility critical exponent is zero. When λ is larger than the critical value, the system undergoes a first-order phase transition at finite contagion rate. As λ approaches the critical value λ_c from above ($\lambda > \lambda_c$), the epidemic threshold converges to a value different from that of $\lambda = \lambda_c$. The susceptibility diverges in the vicinity of the phase transition. The order parameter critical exponent is 1/2 and the susceptibility critical exponent is positive.

We believe that the mean-field theoretical results are exact in annealed hypergraphs. However, for quenched hypergraphs, the epidemic threshold must be investigated for larger systems, because the mean-field theory led to a misleading prediction for the epidemic threshold in quenched scale-free network [26]. Possible logarithmic decay of the density of infection, which is characterized as the Griffiths phase [27], must also be checked.

3.2.1 Self-consistency equation

The infection probability of degree-k nodes ρ_k satisfies the following mean-field differential equation.

$$\frac{1}{\mu}\frac{d}{dt}\rho_k = -\rho_k + \eta k\,(1-\rho_k)\,\Theta^{d-1}, \tag{3.12}$$

where $\eta = \beta/\mu$, and Θ is the portion of $k(d-1)$ neighbors that are infected. Then, Θ is the k-weighted average of infection probability:

$$\Theta = \frac{\sum_{k=m}^{\infty} kP(k)\rho_k(t)}{\sum_{k=m}^{\infty} kP(k)}. \tag{3.13}$$

It is expected that $\Theta^{d-1}k$ among k hyperedges have $d-1$ infected nodes except the degree-k node. The degree-k node is cured ($I \to S$) by rate μ if the node is infected. If the degree-k node is not infected and has n hyperedges that have $d-1$ infected nodes except the degree-k node, the node is infected by rate βn. Since Θ is the weighted average of a quantity larger than zero and smaller than 1: $0 \leq \Theta \leq 1$. We are interested in the stationary states, therefore we set $\mu = 1$ without loss of generality. This is equivalent to the transform $t \to \mu t$, which does not affect the stationary ensemble.

The stationary solution for ρ_k is obtained when $\frac{d}{dt}\rho_k = 0$ for all k:

$$\rho_k = \frac{\eta k \Theta^{d-1}}{1 + \eta k \Theta^{d-1}}. \tag{3.14}$$

The equation implies that the infection probability always increases with the node's degree and approaches 1 as $k \to \infty$ for any positive η and Θ. The function ρ_k is controlled by a single parameter $\eta\Theta^{d-1}$. The density of infection, which is the overall probability of infection, is $\rho = \sum P(k)\rho_k$, and monotonically increases with Θ and satisfies $0 \leq \rho \leq 1$. Non-zero $\eta\Theta^{d-1}$ implies a non-zero ρ_k and ρ. ρ is always less than or equal to Θ, because Θ is the degree weighted average of ρ_k and ρ_k increases with k.

The self-consistency equation for Θ is obtained by introducing ρ_k expressed in Eq. 3.14 to Eq. 3.13.

$$\Theta = \frac{1}{\langle k \rangle} \sum_k kP(k)\rho_k = \frac{1}{\langle k \rangle} \sum_k kP(k) \frac{\eta k \Theta^{d-1}}{1 + \eta k \Theta^{d-1}} \tag{3.15}$$

where $\langle k \rangle$ is the average degree of the hypergraph. Define self-consistency function

$G(\Theta)$ as

$$G(\Theta) = \frac{1}{\langle k \rangle} \sum_k kP(k) \frac{\eta k \Theta^{d-1}}{1 + \eta k \Theta^{d-1}} - \Theta \tag{3.16}$$

$G(\Theta_0) = 0$ yields the Θ_0 value that corresponds to the stationary solution. In order to carry out calculations explicitly, we use a continuous-k approximation. We replace the summation $\sum_{k=k_m}^{\infty} P(k)$ by an integration $\int_{k_m}^{\infty} dkP(k)$. The self-consistency function becomes,

$$G(\Theta) = \frac{1}{\langle k \rangle} \int_{k_m}^{\infty} dkkP(k) \frac{\eta k \Theta^{d-1}}{1 + \eta k \Theta^{d-1}} - \Theta. \tag{3.17}$$

For power-law degree distribution $P(k) = (\lambda - 1) k_m^{\lambda-1} k^{-\lambda}$, $k \geq m$,

$$G(\Theta) = (\lambda - 2) k_m^{\lambda-2} \int_{k_m}^{\infty} dk \frac{\eta k^{-\lambda+2} \Theta^{d-1}}{1 + \eta k \Theta^{d-1}} - \Theta \tag{3.18}$$

$$G(\Theta) = {}_2F_1 \left(\lambda - 2, 1; \lambda - 1; -\frac{1}{k_m \eta \Theta^{d-1}} \right) - \Theta, \tag{3.19}$$

where ${}_2F_1(a, b; c, z)$ is the Gauss hypergeometric function defined

$${}_2F_1(a, b; c, z) = \frac{\Gamma(c)}{\Gamma(a)\Gamma(b)} \sum_{n=0}^{\infty} \frac{\Gamma(a+n)\Gamma(b+n)}{\Gamma(c+n)} \frac{z^n}{n!} \tag{3.20}$$

[78]. The density of infection ρ is expressed,

$$\rho = \int_{k_m}^{\infty} dkP(k) \frac{\eta k \Theta^{d-1}}{1 + \eta k \Theta^{d-1}} = {}_2F_1 \left(\lambda - 1, 1; \lambda; -\frac{1}{k_m \eta \Theta^{d-1}} \right). \tag{3.21}$$

The continuous-k approximation becomes exact for large k_m and for annealed hypergraphs (see section 4.1.3 for the definition). The self-consistency function has the following properties.

$$G(0) = 0 \tag{3.22}$$

$$G(1) = \frac{1}{\langle k \rangle} \int_{k_m}^{\infty} dk k P(k) \frac{\eta k}{1+\eta k} - 1 < 0 \tag{3.23}$$

$$G'(\Theta) = \frac{\lambda - 2}{k_m^{-\lambda+2}} \int_{k_m}^{\infty} dk \left(\frac{(d-1)\eta k^{-\lambda+2}\Theta^{d-2}}{1+\eta k \Theta^{d-1}} - \frac{(d-1)\eta^2 k^{-\lambda+3}\Theta^{2d-3}}{(1+\eta k \Theta^{d-1})^2} \right) - 1. \tag{3.24}$$

Therefore, $G'(0) = -1$ for $d > 2$. However, we are dealing with infinite summations and integrations, hence the limits of $G(\Theta)$ and $G'(\Theta)$ must also be checked for $\Theta \to 0$.

$$\lim_{\Theta \to 0} G(\Theta) = G(0) = 0 \tag{3.25}$$

$$G'(\Theta) = \frac{(d-1)(\lambda-2)}{k_m \eta \Theta^d (\lambda - 1)} {}_2F_1 \left(\lambda - 1, 2; \lambda; -\frac{1}{k_m \eta \Theta^{d-1}} \right) - 1. \tag{3.26}$$

By using an identity

$$\begin{aligned} {}_2F_1(a,b;c;-z) = & \frac{z^{-a}\Gamma(c)\Gamma(b-a)}{\Gamma(b)\Gamma(c-a)} {}_2F_1\left(a, a-c+1; a-b+1; -\tfrac{1}{z}\right) \\ & + \frac{z^{-b}\Gamma(c)\Gamma(a-b)}{\Gamma(a)\Gamma(c-b)} {}_2F_1\left(b, b-c+1; -a+b+1; -\tfrac{1}{z}\right), \end{aligned} \tag{3.27}$$

we obtain the asymptotic behavior of the hypergeometric function ${}_2F_1(a,b;c;-z)$ for $z \to \infty$:

$${}_2F_1(a,b;c;-z) \sim \begin{cases} \frac{\Gamma(c)\Gamma(b-a)}{\Gamma(b)\Gamma(c-a)} z^{-a} & a < b \\ \frac{\Gamma(c)\Gamma(a-b)}{\Gamma(a)\Gamma(c-b)} z^{-b} & a > b \end{cases}. \tag{3.28}$$

The formula also allows us to calculate the next dominant terms proportional to z^{-a-1}, z^{-a-2}, $\cdots$, and z^{-b-1}, z^{-b-2}, $\cdots$. For $\Theta \to 0$,

$$G'(\Theta) \sim \begin{cases} \frac{\pi(d-1)(\lambda-2)^2}{\sin(\pi\lambda)} (k_m \eta)^{\lambda-2} \Theta^{(d-1)\lambda-(d-1)-d} - 1 & \lambda < 3 \\ \frac{(d-1)(\lambda-2)}{(\lambda-3)} k_m \eta \Theta^{d-2} - 1 & \lambda > 3 \end{cases} \tag{3.29}$$

$$\lim_{\Theta\to 0} G'(\Theta) = \begin{cases} +\infty & \lambda < 2+\frac{1}{d-1} \\ \frac{\pi/(d-1)}{\sin(\pi/(d-1))}\left(k_m\eta\right)^{1/(d-1)} - 1 & \lambda = 2+\frac{1}{d-1} \\ -1 & \lambda > 2+\frac{1}{d-1} \end{cases}. \tag{3.30}$$

The order of the phase transition and the epidemic threshold is governed by the value of $\lim_{\Theta\to 0} G'(\Theta)$. If $\lim_{\Theta\to 0} G'(\Theta) = \infty$, since $G(0) = 0$ and $G(1) < 0$, there is one non-trivial stationary solution Θ_0 that satisfies the self-consistency equation. Therefore, the system has a vanishing epidemic threshold. When $\lim_{\Theta\to 0} G'(\Theta)$ is a monotonically increasing function of η, the self-consistency equation yields one non-trivial stationary solution when η is larger than a critical value. The epidemic threshold for scale-free d-uniform hypergraph with the degree exponent $\lambda = 2+\frac{1}{d-1}$ is $\eta_c(\lambda_c) = \frac{1}{k_m}\left[\frac{\sin(\pi/(d-1))}{\pi/(d-1)}\right]^{d-1}$. The phase transition is of order two. If $\lim_{\Theta\to 0} G'(\Theta)$ is fixed to -1, the system has no non-trivial stationary solution under the epidemic threshold, and two solutions above the threshold. The smaller one is an unstable solution and the larger one is a stable solution. The self-consistency equations of 3- and 4-uniform hypergraphs are plotted for several values of λ in Fig. 3.4.

3.2.2 Fluctuation

We have ignored the effects of the stochastic fluctuation in the system and focused on the expectation values of the physical quantities. In the presence of stochastic noise, the equation for the degree-k nodes is expressed,

$$\frac{d}{dt}\rho_k = -\rho_k + \eta k\left(1-\rho_k\right)\Theta^{d-1} + \zeta_k. \tag{3.31}$$

The origin of the noise is the stochastic nature of the recovery process and the contagion process. We start from the conditional probability of the system. Suppose

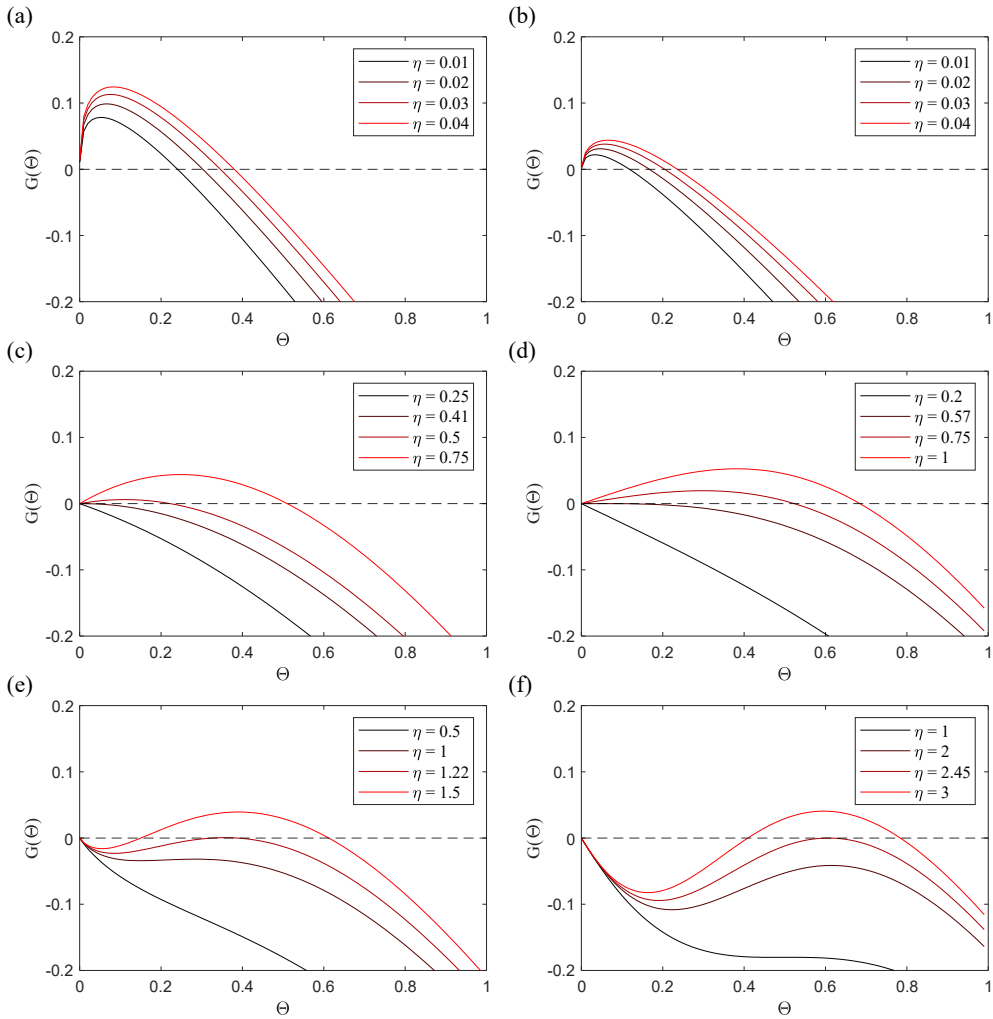

Fig. 3.4: Self-consistency function $G(\Theta)$ of scale-free 3-uniform hypergraphs with degree exponent (a) $\lambda = 2.2$, (c) $\lambda = 2.5$, (e) $\lambda = 2.8$, and of scale-free 4-uniform hypergraphs with degree exponent (a) $\lambda = 2.2$, (c) $\lambda = 2 + 1/3$, (e) $\lambda = 2.8$. The minimum expected degree $k_m = 1$. For $\lambda < \lambda_c$, the derivative of the function diverges as Θ approaches zero ((a) and (b)). For $\lambda = \lambda_c$, it converges to a finite value according to the value of the rate of contagion η ((c) and (d)). For $\lambda > \lambda_c$, it converges to -1 regardless of η ((e) and (f)).

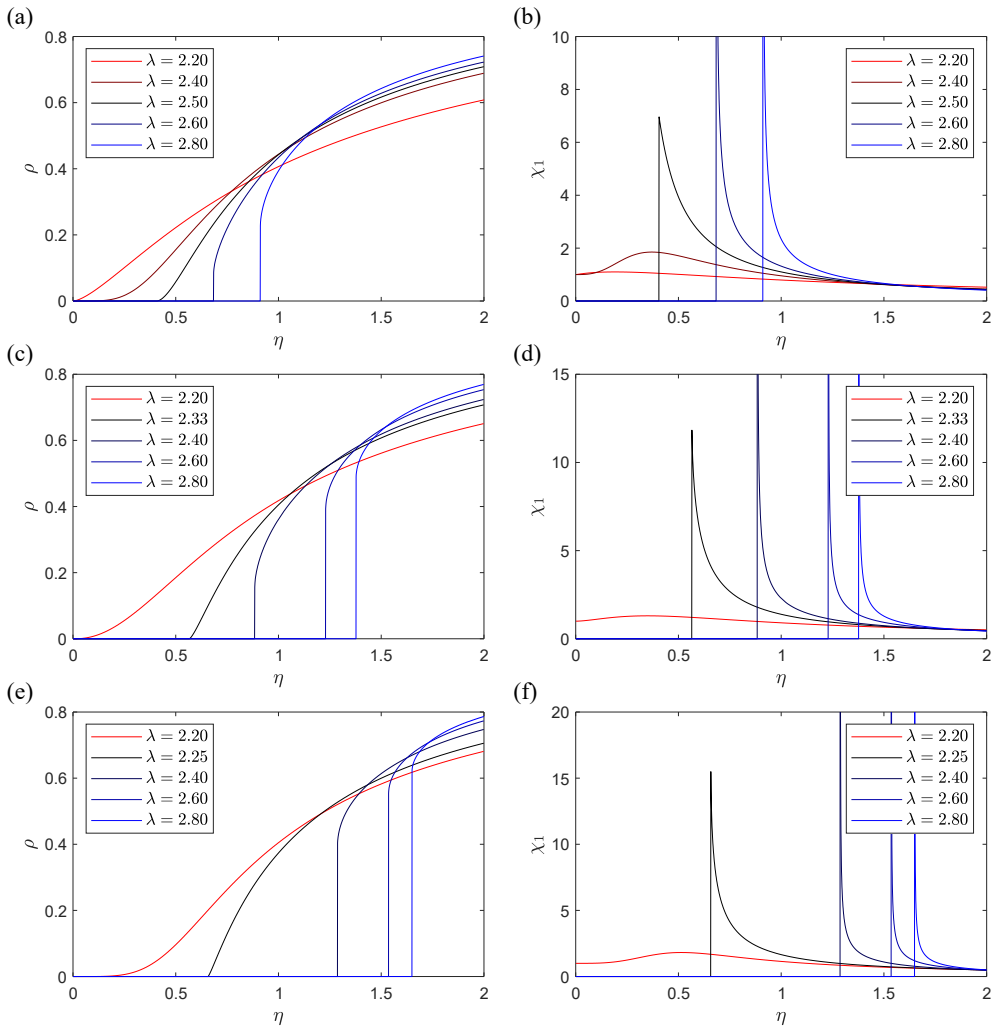

Fig. 3.5: Mean-field theoretical results of (a, c, e) the density of infection and (b, d, f) the susceptibility. The mean degree $\langle k \rangle = d$, which corresponds to $K = 1$ in the static model. Red lines denote $\lambda < \lambda_c$, blue lines denote $\lambda > \lambda_c$, and black lines denote $\lambda = \lambda_c$. For $\lambda < \lambda_c$, the epidemic threshold vanishes. The susceptibility converges to 1 as $\eta \to 0$. For $\lambda = \lambda_c$, the epidemic threshold is finite and the system undergoes a second-order phase transition where the density of infection is continuous in the vicinity of the phase transition. The susceptibility converges to a finite value $1 + d(d-2)$. For $\lambda > \lambda_c$, the phase transition is of first-order and the density of infection is discontinuous in the vicinity of the phase transition. The susceptibility diverges in the vicinity of the phase transition.

that there are $N_k\rho_k$ infected degree-k nodes. Then the probability that n_1 nodes are cured in duration dt is given,

$$P(n_1) = \binom{N_k\rho_k}{n_1} (dt)^{n_1} (1-dt)^{N\rho-n_1}. \tag{3.32}$$

There are approximately $N_k k (1-\rho_k) \Theta^{d-1}$ attempts of infection in the system. The probability that n_2 nodes are infected in duration dt is

$$P(n_2) = \binom{N_k k (1-\rho_k) \Theta^{d-1}}{n_2} (\eta dt)^{n_2} (1-\eta dt)^{N\Theta^{d-1}-N\Theta^d-n_2}. \tag{3.33}$$

Then, the conditional probability that the number of infected degree-k nodes N_{kI} increases by n in duration dt can be calculated using the joint probability $P(n_1,n_2)$

$$\begin{aligned} P(N_{k\mathrm{I}}+n,t+dt|N_{k\mathrm{I}},t) &= \sum_{n_1=0}^{N_k k(1-\rho_k)\Theta^{d-1}-n} P(n_1,n+n_1) \\ &= \sum \binom{N_k\rho_k}{n_1} \binom{N_k k (1-\rho_k) \Theta^{d-1}}{n+n_1} (dt)^{n_1} (1-dt)^{N\rho-n_1} \\ &\qquad (\eta dt)^{n+n_1} (1-\eta dt)^{N_k k(1-\rho_k)\Theta^{d-1}-n-n_1}. \end{aligned} \tag{3.34}$$

The dynamics of the system is expressed by the master equation,

$$\frac{\partial}{\partial t} P(\rho_k,t) = \int d\rho' \left[W(\rho_k|\rho_k') P(\rho_k') - W(\rho_k'|\rho_k) P(\rho_k) \right] \tag{3.35}$$

$$W(N_{kI}+n|N_{kI}) = \frac{\partial}{\partial t} P(N_{k\mathrm{I}}+n,t+dt|N_{k\mathrm{I}},t) \tag{3.36}$$

$$= \delta(n-1) \left[N_{k\mathrm{I}} + \eta N_k k (1-\rho_k) \Theta^{d-1} \right]. \tag{3.37}$$

Let $\mu = 1$ for convenience and use Kramers-Moyal expansion to obtain

$$\frac{d}{dt}\rho_k = \alpha_1(\rho_k,t) + \sqrt{\alpha_2}\xi_k, \tag{3.38}$$

where

$$\alpha_1(\rho_k,t) = \int d\rho_k'(\rho_k' - \rho_k)W(\rho_k'|\rho_k) \tag{3.39}$$

$$\alpha_2(\rho_k,t) = \int d\rho_k'(\rho_k' - \rho_k)^2 W(\rho_k'|\rho_k) \tag{3.40}$$

$$\alpha_2 = \frac{\rho_k + N_k k\,(1-\rho_k)\,\Theta^{d-1}}{N_k} \tag{3.41}$$

$$\left\langle \zeta_k(t)\zeta_k(t')\right\rangle = \left(\frac{\rho_k + N_k k\,(1-\rho_k)\,\Theta^{d-1}}{N_k}\right)\delta(t'-t) \tag{3.42}$$

$$\simeq \frac{\left\langle \rho_k + N_k k\,(1-\rho_k)\,\Theta^{d-1}\right\rangle}{NP(k)}\delta(t'-t). \tag{3.43}$$

For stationary state, $\rho_k = N_k k\,(1-\rho_k)\,\Theta^{d-1}$. This means that the rate of recovery and the rate of contagion are equal. Then ζ_k becomes a multiplicative noise.

$$\left\langle \zeta_k(t)\zeta_k(t')\right\rangle = \frac{2\left\langle \rho_k\right\rangle}{NP(k)}\delta(t'-t). \tag{3.44}$$

If we assume that the stochastic noise for two distinct degrees are independent,

$$\frac{d}{dt}\int dkP(k)\rho_k = -\int dkP(k)\rho_k + \eta\int dkkP(k)\,(1-\rho_k)\,\Theta^{d-1} + \int dkP(k)\zeta_k \tag{3.45}$$

$$\frac{d}{dt}\rho = -\rho + \eta \langle k \rangle (1-\Theta)\Theta^{d-1} + \zeta \tag{3.46}$$

$$\langle \zeta(t)\zeta(t') \rangle = \frac{2\langle \rho \rangle}{N}\delta(t'-t). \tag{3.47}$$

The stochastic fluctuation is a multiplicative noise when the system is in a stationary state.

3.2.3 Critical behavior of the density of infection

For $\lambda < \lambda_c$, the epidemic threshold η_c is zero, and both ρ and Θ approaches zero as $\eta - \eta_c = \eta \to 0$. Therefore,

$$G(\Theta; k_m\eta) \simeq \frac{(\lambda-2)\pi}{\sin(\pi\lambda)}\left(k_m\eta\Theta^{d-1}\right)^{\lambda-2} - \Theta \tag{3.48}$$

$$\Theta \sim (k_m\eta)^{\frac{\lambda-2}{1-(d-1)(\lambda-2)}}. \tag{3.49}$$

The density of infection ρ can also be calculated from Eq. 3.21:

$$\rho \sim k_m\eta\Theta^{d-1} \sim (\eta-\eta_c)^{\frac{1}{1-(d-1)(\lambda-2)}}. \tag{3.50}$$

For $\lambda = \lambda_c$, the epidemic threshold $\eta_c = \frac{1}{k_m}\left[\frac{\sin(\pi/(d-1))}{\pi/(d-1)}\right]^{d-1}$ is finite. Both ρ and Θ approaches zero as $\eta - \eta_c \to 0$. The self-consistency function $G(\Theta)$ is expressed as Eq. 3.48. In this case, we have to consider higher order terms of $G(\Theta)$ because there is only $O(\Theta)$ term in the equation. The next two dominant terms of $G(\Theta)$ are $O(\Theta^d)$ arising from the first term of Eq. 3.27 and $O(\Theta^{d-1})$ from the second term. The

latter is more dominant and is also negative.

$$G(\Theta;k_m\eta) = {}_2F_1\left(\frac{1}{d-1},1;1+\frac{1}{d-1};-\frac{1}{k_m\eta\Theta^{d-1}}\right)-\Theta \tag{3.51}$$

$$= \left(\frac{\Gamma(1+\frac{1}{d-1})\Gamma(1-\frac{1}{d-1})}{\Gamma(1)\Gamma(1)}(k_m\eta)^{1/(d-1)}-1\right)\Theta \tag{3.52}$$

$$+\frac{\Gamma(1+\frac{1}{d-1})\Gamma(\frac{1}{d-1}-1)}{\Gamma(\frac{1}{d-1})\Gamma(\frac{1}{d-1})}(k_m\eta)\,\Theta^{d-1}+\cdots \tag{3.53}$$

$$= \frac{\eta-\eta_c}{(d-1)\eta_c}\Theta-\frac{1}{d-2}(k_m\eta_c)\,\Theta^{d-1}+\cdots. \tag{3.54}$$

Therefore,

$$\Theta \sim (\eta-\eta_c)^{\frac{1}{d-2}} \tag{3.55}$$

$$\rho \sim (\eta-\eta_c)^{\frac{d-1}{d-2}}. \tag{3.56}$$

For $\lambda > \lambda_c$, none of η_c, ρ, and Θ approaches zero as $\eta-\eta_c \to 0^+$. We can calculate the asymptotic behavior of $\Theta(\eta)-\Theta(\eta_c)$ and $\rho(\eta)-\rho(\eta_c)$. In the vicinity of the phase transition, $G=0$ and $\frac{\partial G}{\partial\Theta}=0$. Therefore,

$$G(\Theta+\Delta\Theta;k_m\eta+k_m\Delta\eta) = \frac{1}{2}\frac{\partial^2 G}{\partial\Theta^2}(\Delta\Theta)^2+\frac{\partial G}{\partial\eta}\Delta\eta \tag{3.57}$$

$$\Theta(\eta)-\Theta(\eta_c) \sim (\eta-\eta_c)^{1/2} \tag{3.58}$$

$$\rho(\eta)-\rho(\eta_c) \sim (\eta-\eta_c)^{1/2}. \tag{3.59}$$

The density of infection ρ has the same asymptotic behavior with Θ because ρ is not

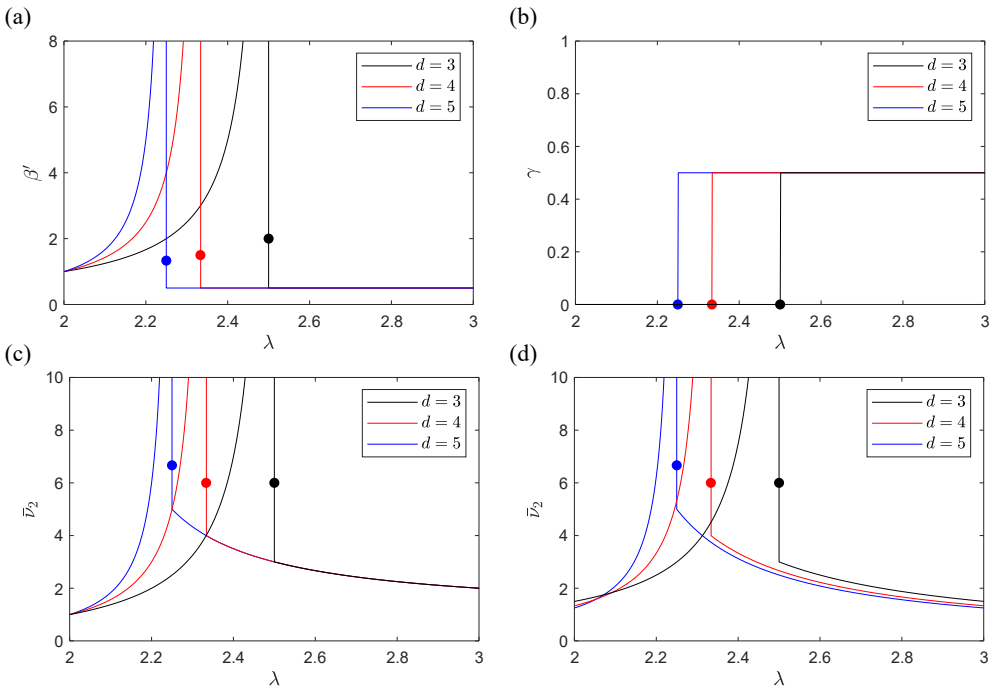

Fig. 3.6: Critical exponents (a) β', (b) γ, and (c, d) $\bar{\nu}_2$. The order parameter critical exponent β' diverges near the critical point λ_c. The correlation length critical exponent of the second kind $\bar{\nu}_2$ is calculated for (c) $\omega = \lambda - 1$, which is the natural cut-off, and for (d) $\omega = d/(d-1)$, which yields uncorrelated scale-free hypergraphs. The two plots (c) and (d) differ and confirm that there are various routes to the thermodynamic limit of scale-free uniform hypergraphs.

singular at the point. Therefore, the order parameter critical exponent β' is given,

$$\beta' = \begin{cases} \frac{1}{1-(d-1)(\lambda-2)} & \lambda < \lambda_c \\ \frac{d-1}{d-2} & \lambda = \lambda_c \\ 1/2 & \lambda > \lambda_c \end{cases} . \tag{3.60}$$

The exponents are illustrated in Fig. 3.6 (a) for $d = 3, 4, 5$.

3.2.4 Susceptibility

There are multiple definitions of susceptibility in SIS model. One was introduced [79, 80] in the context of directed percolation, which is equivalent to SIS-model in regular networks [81]. It is defined under the presence of conjugated field h.

$$\frac{d}{dt}\rho = -\rho + \eta \langle k \rangle (1 - \Theta[\rho]) \Theta[\rho]^{d-1} + h \tag{3.61}$$

$$= f(\rho) + h. \tag{3.62}$$

The conjugated field h is related to the rate $h' = h/(1-\rho)$ of voluntary infection $S \to I$, the rate of which a susceptible node is turned to an infected state independent of the contagion process. The susceptibility χ_1 is defined as the sensitivity of the density of infection to the conjugated field:

$$\chi_1 = \frac{\partial \rho}{\partial h} = \frac{1}{1-\rho} \frac{\partial \rho}{\partial h'}. \tag{3.63}$$

In such case, the differential equation for the infection probability of degree-k nodes is modified as follows.

$$\frac{d}{dt}\rho_k = -\rho_k + \eta k (1 - \rho_k) \Theta^{d-1} + (1 - \rho_k) h' \tag{3.64}$$

$$\rho_k = \frac{h' + \eta k \Theta^{d-1}}{1 + h' + \eta k \Theta^{d-1}} \tag{3.65}$$

$$\rho_k \left(\eta, h'; \Theta\right) = \frac{h'}{1+h'} + \frac{1}{1+h'} \rho_k \left(\frac{\eta}{1+h'}, 0; \Theta \right) \tag{3.66}$$

$$\rho \left(\eta, h'; \Theta\right) = \frac{h'}{1+h'} + \frac{1}{1+h'} \rho \left(\frac{\eta}{1+h'}, 0; \Theta \right). \tag{3.67}$$

The self-consistency equation is modified,

$$\Theta = \frac{1}{\langle k \rangle} \int_{k_m}^{\infty} dk k P(k) \frac{\eta k \Theta^{d-1}}{1 + h' + \eta k \Theta^{d-1}} + \frac{1}{\langle k \rangle} \int_{k_m}^{\infty} dk k P(k) \frac{h'}{1 + h' + \eta k \Theta^{d-1}} \quad (3.68)$$

$$G(\Theta, h') = {}_2F_1\left(\lambda - 2, 1; \lambda - 1; -\frac{1+h'}{k_m \eta \Theta^{d-1}}\right) + h' \frac{\lambda - 2}{\lambda - 1} \frac{1}{k_m \eta \Theta^{d-1}} {}_2F_1\left(\lambda - 1, 1; \lambda; -\frac{1+h'}{k_m \eta \Theta^{d-1}}\right) - \Theta \quad (3.69)$$

$$dG = \left.\frac{\partial G}{\partial \Theta}\right|_{\eta, h'} d\Theta + \left.\frac{\partial G}{\partial h}\right|_{\eta, \Theta} dh' = 0 \quad (3.70)$$

$$(1 - \rho)\chi_1 = \left.\frac{\partial \rho}{\partial h'}\right|_{\eta, \Theta} - \left.\frac{\partial \rho}{\partial \Theta}\right|_{\eta, h'} \left.\frac{\partial G}{\partial h'}\right|_{\eta, \Theta} \left(\left.\frac{\partial G}{\partial \Theta}\right|_{\eta, h'}\right)^{-1}. \quad (3.71)$$

For $\lambda > \lambda_c$, $\frac{\partial G}{\partial \Theta}$ approaches zero as η approaches η_c and the other two factors in Eq. 3.71 are not singular. Hence the susceptibility diverges in the vicinity of the phase transition. For $\lambda \leq \lambda_c$, the other two terms must be taken into account. The derivatives can all be carried out analytically by the mean-field theory.

$$\left.\frac{\partial \rho}{\partial h'}\right|_{\eta, \Theta} = 1 - {}_2F_1\left(\lambda - 1, 1; \lambda; -\frac{1}{k_m \eta \Theta^{d-1}}\right) - \frac{\lambda - 1}{\lambda} \frac{1}{m \eta \Theta^{d-1}} {}_2F_1\left(\lambda, 2; \lambda + 1; -\frac{1}{k_m \eta \Theta^{d-1}}\right) \quad (3.72)$$

$$\left.\frac{\partial \rho}{\partial \Theta}\right|_{\eta, h'} = \frac{(d-1)(\lambda - 1)}{\lambda} \frac{1}{k_m \eta \Theta^d} {}_2F_1\left(\lambda, 2; \lambda + 1; -\frac{1}{k_m \eta \Theta^{d-1}}\right) \quad (3.73)$$

$$\left.\frac{\partial G}{\partial \Theta}\right|_{\eta, h'} = \frac{(d-1)(\lambda - 2)}{\lambda - 1} \frac{1}{k_m \eta \Theta^d} {}_2F_1\left(\lambda - 1, 2; \lambda; -\frac{1}{k_m \eta \Theta^{d-1}}\right) - 1 \quad (3.74)$$

$$\left.\frac{\partial G}{\partial h'}\right|_{\eta,\Theta} = \frac{\lambda-2}{\lambda-1}\frac{1}{k_m\eta\Theta^{d-1}}\left[{}_2F_1\left(\lambda-1,1;\lambda;-\frac{1}{k_m\eta\Theta^{d-1}}\right)\right.$$
$$\left. - {}_2F_1\left(\lambda-1,2;\lambda;-\frac{1}{k_m\eta\Theta^{d-1}}\right)\right]. \quad (3.75)$$

The values are calculated for $h'=0$. The susceptibility is then expressed,

$$(1-\rho)\,\chi_1 = 1 - {}_2F_1\left(\lambda-1,1;\lambda;-\frac{1}{k_m\eta\Theta^{d-1}}\right)$$
$$-\frac{\lambda-1}{\lambda}\frac{1}{k_m\eta\Theta^{d-1}}{}_2F_1\left(\lambda,2;\lambda+1;-\frac{1}{k_m\eta\Theta^{d-1}}\right)$$
$$-\frac{(d-1)(\lambda-2)}{\lambda k_m^2\eta^2\Theta^{2d-1}}\frac{{}_2F_1\left(\lambda,2;\lambda+1;-\frac{1}{k_m\eta\Theta^{d-1}}\right)}{\frac{(d-1)(\lambda-2)}{\lambda-1}\frac{1}{k_m\eta\Theta^d}{}_2F_1\left(\lambda-1,2;\lambda;-\frac{1}{k_m\eta\Theta^{d-1}}\right)-1}$$
$$\left[{}_2F_1\left(\lambda-1,1;\lambda;-\frac{1}{k_m\eta\Theta^{d-1}}\right) - {}_2F_1\left(\lambda-1,2;\lambda;-\frac{1}{k_m\eta\Theta^{d-1}}\right)\right]. \quad (3.76)$$

The susceptibility χ_1 is illustrated in Fig. 3.5 for $d=3,4,5$. Eq. 3.76 allows us to calculate the susceptibility critical exponent γ: $\chi_{\mathrm{DP}} \sim (\eta-\eta_c)^{-\gamma}$.

$$\gamma = \begin{cases} 0 & \lambda < \lambda_c \\ 0 & \lambda = \lambda_c \\ 1/2 & \lambda > \lambda_c \end{cases}. \quad (3.77)$$

The results are depicted in Fig. 3.6 (b) for $d=3,4,5$. For $\lambda<\lambda_c$, the susceptibility critical exponent γ is zero and the susceptibility χ_1 converges to 1 in the vicinity of the phase transition. For $\lambda=\lambda_c$, the susceptibility converges. The higher order terms of $\left(\left.\frac{\partial G}{\partial\Theta}\right|_{\eta,h'}\right)^{-1}$ must be taken into account to calculate γ in this case. The converging

susceptibility is given,

$$\chi_1(\eta_c;\lambda_c) = 1 + \frac{(\lambda_c - 1)(3 - \lambda_c)}{(\lambda_c - 2)^2} = 1 + d(d-1). \tag{3.78}$$

Another definition of the susceptibility has been introduced for an effective determination of the epidemic threshold in numerical simulations of SIS-model in finite-size heterogeneous networks [82]. It is defined

$$\chi_2 = N\frac{\langle \rho^2 \rangle - \langle \rho \rangle^2}{\langle \rho \rangle}. \tag{3.79}$$

We calculate both the χ_1 and χ_2 in the numerical simulations.

3.2.5 Finite-size effect

There are two types of finite-size effect in scale-free networks [83]. The same is true in scale-free uniform hypergraphs. The finite-size effect of the first kind originates from the fact that the number of nodes in the system is finite. It is the same kind of finite-size effect studied in regular lattices. Because of this effect, a stationary state in any finite-size system has a finite life-time. The finite-size effect of the second kind stems from the fact that the maximum degree in a finite system is always finite. The maximum degree of a finite-size uniform hypergraph can never be infinite, whether the hypergraph is weighted or unweighted. Especially in an unweighted d-uniform hypergraph, it is bounded by ${}_{N-1}C_{d-1}$, which is the number possible distinct hyperedges of size d that contains a specific node. Therefore, a finite maximum degree is inevitable in a finite system. The thermodynamic limit of scale-free uniform hypergraphs must take both the $N \to \infty$ and $k_{\max} \to \infty$ limits. The finite-size effect of the second kind differs from the first kind because the epidemic threshold is defined

for each value of $k_{\max}$. Therefore, the effect depends on the exponent of which the $k_{\max}$ diverges. If we fix the $k_{\max}$ and increase the number of nodes, we can study the finite-size effect of the first kind exclusively. If we increase the maximum degree with sufficiently small exponent, the finite-size effect of the first kind will vanish first, and only the finite-size effect of the second kind will remain.

In the static model, the maximum expected degree diverges with an exponent $\frac{1}{\lambda-1}$, which is called the natural cut-off of the static model [59]. However, we can control the exponent with an arbitrary value. We assign p_i on each node with probability

$$p_i = \frac{\left(1+\frac{N^{(\lambda-1)/\omega}-1}{N-1}(i-1)\right)^{-\mu}}{\sum_{j=1}^{N}\left(1+\frac{N^{(\lambda-1)/\omega}-1}{N-1}(j-1)\right)^{-\mu}} \tag{3.80}$$

instead of Eq. 2.4. The exponent of the degree distribution is $\lambda = 1+\frac{1}{\mu}$, and maximum value of p_i is

$$\max(p_i) = \left[\sum_{j=1}^{N}\left(1+\frac{N^{(\lambda-1)/\omega}-1}{N-1}(j-1)\right)^{-\mu}\right]^{-1} \tag{3.81}$$

$$\simeq \left(N^{-\frac{(\lambda-1)\mu}{\omega}+1}\int_0^1 dx x^{-\mu}\right)^{-1} \tag{3.82}$$

$$\sim N^{\frac{1}{\omega}-1}. \tag{3.83}$$

Therefore, if $\omega > \frac{d}{d-1}$, $\max\left(d!NKp_{i_1}\cdots p_{i_d}\right) \sim N^{1+d(\omega+1)/\omega} \to 0$ and the probability of hyperedge is expressed by Eq. 2.10: $f_{i_1\cdots i_d} \simeq d!NKp_{i_1}\cdots p_{i_d}$ regardless of the degree exponent λ. The minimum degree converges to the same value as the static model and the maximum degree diverges as $k_{\max} \sim N^{1/\omega}$. $\omega = \lambda - 1$ yields the static model.

The self-consistency equation of the model is

$$G_N(\Theta) = \frac{\lambda-2}{m^{-\lambda+2}} \int_{k_m}^{k_m N^{1/\omega}} dk \frac{\eta k^{-\lambda+2}\Theta^{d-1}}{1+\eta k \Theta^{d-1}} - \Theta \tag{3.84}$$

$$= G(\Theta) - N^{-(\lambda-2)/\omega}{}_2F_1\left(\lambda-2,1;\lambda-1;-\frac{1}{k_m N^{1/\omega}\eta\Theta^{d-1}}\right), \tag{3.85}$$

whose solution yields the degree weighted mean of the density of infection in a finite-size system. The function is illustrated in Fig. 3.7 (a), (b), and (c). $G_N(\Theta)$ allows us to calculate the epidemic threshold of finite-size systems and the critical exponent $\bar{\nu}_2$ of which the epidemic threshold converges to its thermodynamic limit (the subscript 2 denotes that the value accounts for the finite-size effect of the second kind). The epidemic threshold of finite-size static model is illustrated in Fig. 3.7 (d).

For $\lambda < 2 + \frac{1}{d-1}$, $\eta \to 0$ and $\Theta \to 0$ at the critical point. Therefore, for large N, in the vicinity of the phase transition,

$$G(\Theta) \simeq (k_m\eta)^{\lambda-2}\Theta^{(d-1)(\lambda-2)} - \Theta, \tag{3.86}$$

and

$$N^{-(\lambda-2)/\omega}{}_2F_1\left(\lambda-2,1;\lambda-1;-\frac{1}{k_m N^{1/\omega}\eta\Theta^{d-1}}\right) \simeq N^{-(\lambda-2)/\omega}, \tag{3.87}$$

since the hypergeometric function converges rapidly to 1. The finite-size epidemic threshold is given when the maximum value of the function Eq. 3.86 is equal to Eq. 3.87. Therefore,

$$\eta_c(N) \sim N^{-(1-(d-1)(\lambda-2))/\omega}. \tag{3.88}$$

The correlation length critical exponent is $\bar{\nu}_2 = (1-(d-1)(\lambda-2))/\omega$, which ap-

proaches zero as $\lambda \to \lambda_c$. For $\lambda = \lambda_c$, $(\eta - \eta_c) \to 0$ and $\Theta \to 0$ with $\eta_c > 0$. The self-consistency function in the vicinity of the phase transition is

$$G_N(\Theta) = A\,(\eta - \eta_c)\,\Theta - B\Theta^{d-1} - N^{-(\lambda-2)/\omega}, \tag{3.89}$$

where A and B are some positive constant (Eq. 3.54). Therefore,

$$(\eta - \eta_c) \sim N^{-\frac{d-2}{(d-1)^2\omega}}. \tag{3.90}$$

The correlation length critical exponent of the finite-size effect of the second kind is $\bar{\nu}_2 = \frac{(d-1)^2\omega}{d-2}$. For $\lambda > \lambda_c$, $(\eta - \eta_c) \to 0$ and $\Theta - \Theta_c \to 0$ with $\eta_c > 0$ and $\Theta_c > 0$. The finite-size self-consistency function is

$$G_N(\Theta) = G(\Theta) + \frac{\partial G}{\partial \eta}\,(\eta - \eta_c) - N^{-(\lambda-2)/\omega}. \tag{3.91}$$

Therefore,

$$(\eta - \eta_c) \sim N^{-\frac{\lambda-2}{\omega}}. \tag{3.92}$$

The correlation length critical exponent is $\bar{\nu}_2 = \frac{\omega}{\lambda-2}$. The results for $d = 3,4,5$ are illustrated in Fig. 3.6 (c) and (d) for $\omega = \lambda - 1$ and $\omega = d/(d-1)$.

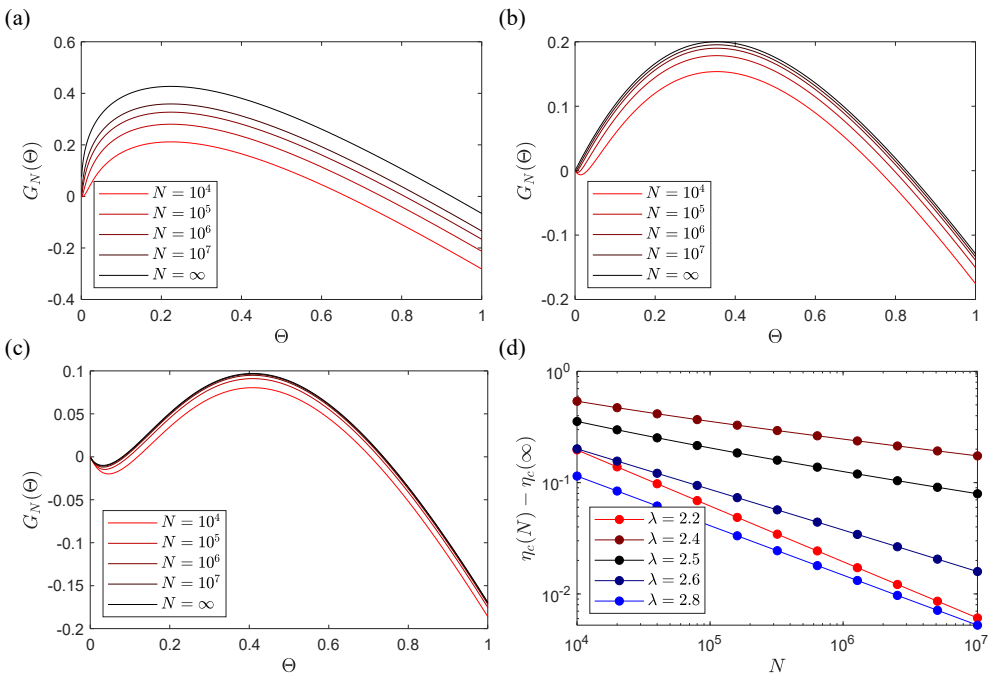

Fig. 3.7: The (a, b, c) self-consistency function and the (d) epidemic threshold of finite-size static model of 3-uniform hypergraph with various exponents of the degree distribution. The maximum expected degree exponent is the natural cut-off $\lambda - 1$.

Chapter 4

Numerical simulation

4.1 Numerical methods

4.1.1 Discretization of time

While the states (S and I) of the agents in the model, and the structure of the position of the agents are discrete, the time of the dynamics is continuous. To simulate such model, one method is to take a small Δt and implement the Newtonian method. At each step, an event of rate α occurs with probability $\alpha\Delta t$. The error of this model is proportional to $\alpha - 1 + \exp(-\alpha\Delta t)$ [84]. Also, the number of times of the random number generation is inversely proportional to Δt, therefore, the simulation time increases.

We used an alternative, computationally efficient method. A cycle of the method is described in the following.

1. Generate a random number X uniformly distributed in $(0,1)$. If $X > p = \frac{\eta}{1+\eta}$, select a random node and recover the node if it is infected.

2. Otherwise (if $X \leq p$), select a random hyperedge and infect the susceptible node in the hyperedge if the hyperedge satisfies the contagion condition.

3. Proceed time t by $\frac{1}{1+\eta}$ ($t \to t + \frac{1}{1+\eta}$).

The simulation is performed by repeating the above cycle.

This algorithm has the same transition probability with the exact continuous-

time model. A given system transforms to a different state by a recovery or an infection of a single node. In the actual system, the rate of the recovery of each node is 1 and the rate of contagion through a hyperedge that satisfies the contagion condition (all nodes in the hyperedge except one are infected) is η. Therefore, the probability that the transition occurs by a recovery of an infected node is $\frac{N_\mathrm{I}}{N}\left(\frac{N_\mathrm{I}}{N}+\eta\frac{n_\mathrm{c}}{n}\right)^{-1}$ and the probability that the transition occurs by a contagion through a hyperedge is $\eta\frac{n_\mathrm{c}}{n}\left(\frac{N_\mathrm{I}}{N}+\eta\frac{n_\mathrm{c}}{n}\right)^{-1}$, where N_I is the number of infected nodes, n is the number of the hyperedges, and n_c is the number of the hyperedges that satisfies the contagion condition. The algorithm presented above gives the identical probability. At each cycle, a recovery is tried by probability $1-p$. The probability that the trial succeeds is N_I/N. The probability that a contagion is tried is p and the probability that the trial succeeds is n_c/n. If the trial fails, the process is repeated to find the state that comes next to the given state. The probability that the system eventually transforms by a recovery or a contagion is then,

$$
\begin{aligned}
P(\text{recovery}) &= (1-p)\frac{N_\mathrm{I}}{N}\sum_{i=0}^{\infty}\left(1-(1-p)\frac{N_\mathrm{I}}{N}-p\frac{n_\mathrm{c}}{n}\right)^{i} && (4.1)\\
&= (1-p)\frac{N_\mathrm{I}}{N}\left((1-p)\frac{N_\mathrm{I}}{N}+p\frac{n_\mathrm{c}}{n}\right)^{-1} && (4.2)\\
&= \frac{N_\mathrm{I}}{N}\left(\frac{N_\mathrm{I}}{N}+\eta\frac{n_\mathrm{c}}{n}\right)^{-1} && (4.3)\\
P(\text{contagion}) &= \eta\frac{n_\mathrm{c}}{n}\left(\frac{N_\mathrm{I}}{N}+\eta\frac{n_\mathrm{c}}{n}\right)^{-1} && (4.4)\\
&= 1-P(\text{recovery}) && (4.5)
\end{aligned}
$$

The probabilities of the transitions are identical to those of the exact continuous-time model.

Therefore, the probability that a series of states $\{\mathrm{S},\mathrm{I},\mathrm{I},\cdots\}$, $\{\mathrm{S},\mathrm{S},\mathrm{I},\cdots\}$, $\cdots$ is

realized in the exact model and the given simulation method are the same. However, the temporal dynamics are not exactly the same. The transition time from a given state to a different state follows an exponential distribution, since it is a Markov process.

$$\delta t \sim \exp\left(\left(\frac{N_{\mathrm{I}}}{N}+\eta\frac{n_{\mathrm{c}}}{n}\right)^{-1}\right) \tag{4.6}$$

However, in the simulation by the given method, such distribution is approximated.

$$P\left(\delta t=\frac{s}{1+\eta}\right)=\left((1-p)\frac{N_{\mathrm{I}}}{N}+p\frac{n_{\mathrm{c}}}{n}\right)\left(1-(1-p)\frac{N_{\mathrm{I}}}{N}-p\frac{n_{\mathrm{c}}}{n}\right)^{s-1}. \tag{4.7}$$

The probability distribution of δt is still an exponential function, but δt is discretized by $1/(1+\eta)$. For a large enough time-scale, however, the simulation is approximately equivalent to the exact model. The probability that b transitions take time T approximately follows a Gaussian distribution for large b and T, because the duration T is a sum of many exponential variables. The standard deviation of the distribution diverges but the ratio of it to the expectation value converges to 0. Therefore, the simulation method yields identical critical exponents. Also, the ensemble of stationary state is exactly the same.

Similar methods have been used in previous studies. These methods select an infected node and infect a neighbor by probability p and otherwise (by probability $1-p$), recovers an infected node. Such method is effective to simulate the contact process or epidemic models in regular structures. To implement this method to SIS model in heterogeneous structure, an infected node must be selected with probability proportional to its degree. It is computationally inefficient. Degree-weighted selection of nodes is efficiently implemented by the alias method (often called the Robin Hood method) [85]. This method constructs an alias table, and then efficiently selects a node

with the given relative probabilities. The list of infected nodes changes constantly, therefore the alias table must be constructed after each transition of the system.

4.1.2 Quasistationary method

A Markov process with an absorbing state (that is accessible) in a finite-size system (system whose total number of states is finite) is destined to reach the absorbing state. If the system has a non-zero probability to reach the absorbing state after some duration, the probability that the system remains active decreases exponentially, and therefore converges to zero. The standard numerical procedure to investigate the stationary state of the finite-sized system with an absorbing state is by using simulation samples restricted only to surviving runs after sufficiently long time [86]. Such method is not computationally efficient, because the samples that have reached the absorbing state cannot be used to calculate the statistical properties of the stationary state.

An alternative method is the quasistationary method [82, 87], which restricts the system to active states. In this method, if the system reaches the absorbing state, the system is reverted to an active configuration taken randomly from the history of the simulation. Initially, the system is fully infected, because we want to investigate the presence of non-trivial stationary state. After sufficiently long time, the system and the history of the configurations simultaneously reach the stationary ensemble. Therefore, if the system reaches the absorbing state by a small probability, the system is immediately reverted to the active state chosen randomly from the stationary ensemble.

For the simulation in this thesis, the number of histories tracked is 100, and the history is updated with period $\frac{1}{\mu} = 1$. When the system reaches the absorbing state, a

configuration from the history is selected randomly and the system is reverted to the chosen configuration.

4.1.3 Annealed uniform hypergraphs

An *annealed hypergraph* is a mean-field theoretical treatment of an ensemble of hypergraphs. We replace the adjacency tensor to its ensemble average:

$$a_\alpha = \bar{a}_\alpha = f_{i_1 \cdots i_d}. \tag{4.8}$$

The probability of a particular hyperedge $f_{i_1 \cdots i_d}$ of the static model of uniform hypergraph was introduced in section 2.3.2. Ordinary hypergraphs, whose neighboring structures are fixed, are called *quenched hypergraphs*. In contrast to quenched hypergraphs, there is no neighboring structure in annealed hypergraphs. There is no disorder in the structure of the annealed hypergraphs, but only in the dynamical processes that take place on them. This is a generalization of the annealed network. Annealed network, which was introduced as a random neighboring network [83], has been widely used to study dynamical processes because degree based mean-field theory and other mean-field theoretical approaches are exact in annealed networks [25, 87–89].

In order to check the mean-field theoretical predictions presented in the previous section, we performed numerical simulations in annealed scale-free 3- and 4-uniform hypergraphs. We used the system size N from 1×10^4 to 4096×10^4. We performed the simulation in the region $2 < \lambda < 3$, a region where the system shows various types of phase transition. We calculated the density of infection and the susceptibility. We calculated the susceptibility by using linear regression of the density of infection under small conjugated field (h between 0.0001 and 0.001). Numerical results

corroborated the mean-field theoretical predictions presented in the previous section.

4.2 Numerical results in annealed 3- and 4-uniform hypergraphs

4.2.1 Temporal dynamics

As explained in the previous section, the dynamics in a finite-size system is destined to reach the absorbing state $\rho(t) = 0$. However, systems with stationary states differ from those without in their temporal dynamics. For instance, the time τ that a system which started from the fully-infected state reaches the absorbing state scales differently as the system size N is increased. The typical time τ' that a stochastic system with Gaussian noise proportional to temperature T, $\langle \zeta(t)\zeta(t') \rangle \propto T\delta(t'-t)$, crosses a potential barrier scales exponentially as $1/T$ increases ($\tau \sim \exp(\Delta E/T)$ for an energy barrier of ΔE) [90]. In this case, $T \propto N^{-1/2}$. Therefore, the typical time of escape from a stationary state scales as $\exp\left(a\sqrt{N}\right)$. The characteristic time τ that a system which started from the fully-infected state reaches the absorbing state scales identically (If the system has a stationary state, the system will spend most of the time in the stationary state, because the time of escape scales faster than a power-law.). However, the characteristic time diverges as a power-law in systems without a stationary state.

We performed numerical simulations for systems with the number of nodes 1250–640000. The survival probability after time t is depicted in Fig. 4.8, at various phases of the system (phase with and without a stationary state, and at the critical point). The characteristic time of survival, which is a typical time that survival probability reaches a certain value, scales as a power-law at or below the critical point. It

diverges faster than a power-law in the phase with a stationary state.

Although any sample of simulation reaches the absorbing state after a sufficiently long time, the average density of infection of the systems that have not reached the absorbing state converges to the stationary value, if there is a stationary state. If there isn't a stationary state, the value indefinitely approaches zero. The results are depicted in Fig. 4.9. Therefore, the stationary state properties can be studied by taking only the surviving samples in the average. The time of relaxation from the fully-infected state is sufficient if if it is larger than 100.

4.2.2 Density of infection

We calculated the density of infection, which is the order parameter of the system, using the quasistationary method introduced in the previous section. We simulated the static model with the natural degree cut-off exponent $\lambda - 1$ with the number of nodes from 1×10^4 to 1024×10^4. We saved $M = 100$ previous configurations (from $t - 100$ to $t - 1$). This differs from the original quasistationary method [82, 87], which replaces a randomly selected history of configuration by a constant rate. The system is initially fully infected. If the system reaches the absorbing state, the system is reverted to a configuration from the history if $t \geq M = 100$. Otherwise, the system is reverted to the fully-infected state. We collected the density infection with a period $\frac{1}{\mu} = 1$, which is the period the history is updated. We used the relaxation time of 2000, hence burned-in the initial 2000 collected data. We used 18000 samples for each system (each N and η) to calculate the mean and the variance of the density of infection.

The results are consistent with the mean-field theoretical predictions and approaches to the prediction as the system size grows. The order of the phase transition

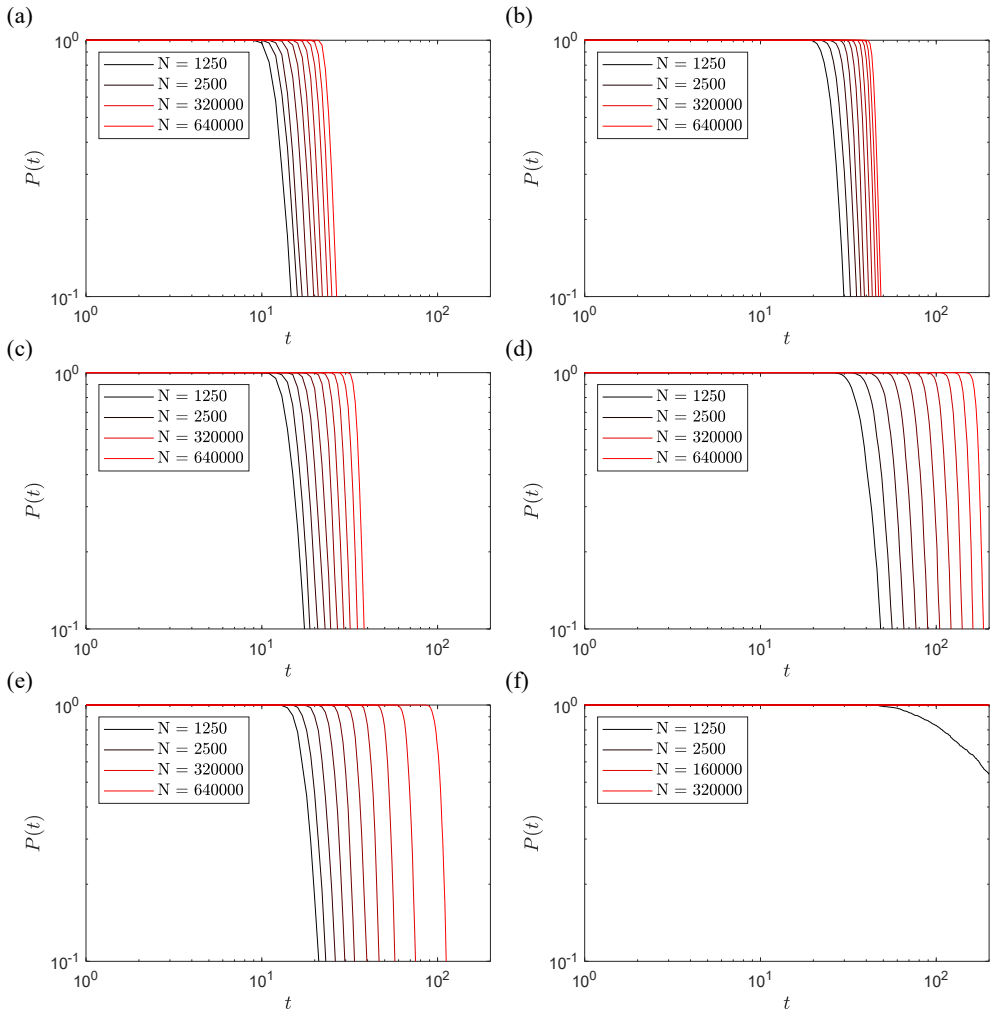

Fig. 4.8: Survival probability at time t of 3-uniform hypergraphs with degree exponent (a, c, e) $\lambda = 2.5$, (b, d, f) $\lambda = 2.8$. The mean degree $\langle k \rangle = d$, which corresponds to $K = 1$ in the static model of uniform hypergraph. The system has a contagion rate below the epidemic threshold, hence there is no stationary state in (a) $\eta = 0.3$ and (b) $\eta = 0.8$. The contagion rate is above the threshold, hence there is a stationary state in (e) $\eta = 0.5$ and (f) $\eta = 1.0$. The systems have the contagion rate equal to the epidemic threshold in (c) and (d). The system is initially fully infected. The characteristic time of survival, the time that the survival probability reaches a certain value, scales as a power-law in (a), (b), (c), (d) and (e). It scales faster than the power-law in (e) and (f), as expected.

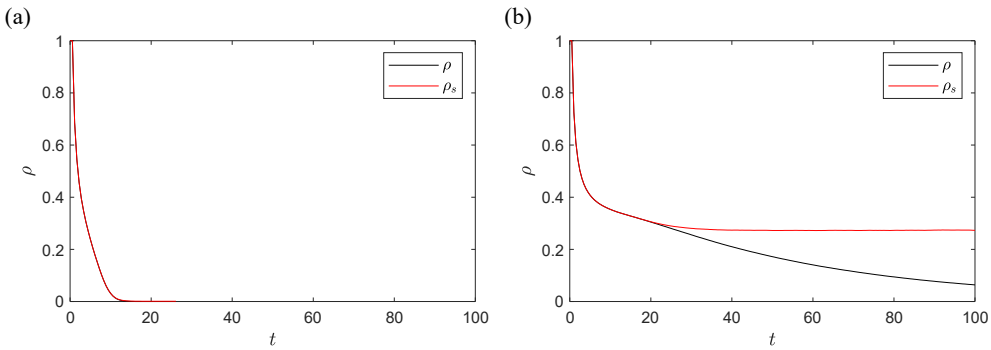

Fig. 4.9: The average density of infection of all runs (black line) and of the surviving runs of scale-free 3-uniform hypergraph with degree exponent $\lambda = 2.8$ and the number of nodes $N = 1000$. The mean degree $\langle k \rangle = d$, which corresponds to $K = 1$ in the static model of uniform hypergraph. The system is below the epidemic threshold in (a) $\eta = 0.8$ and above the threshold in (b) $\eta = 1.0$. The systems are initially fully infected. In both cases, the survival probability approaches zero as time grows, hence the average density of infection of all runs, which is smaller than the survival probability, also approaches zero. However, when the system has a stationary state ((b)), the average density of infection of the surviving runs converges to a finite value, while it approaches zero (a) below the epidemic threshold.

appeared to confirm its mean-field predictions. For $\lambda > 2.5$, where the phase transition is expected to be of first-order, the jump of the order parameter at the epidemic threshold approached a finite value. However, for $\lambda \leq 2.5$, where the phase transition is expected to be of second-order, the jump of the order parameter approached zero. The numerical result of the density of infection is depicted in Fig. 4.10 (3-uniform hypergraph) and Fig. 4.11 (4-uniform hypergraph).

4.2.3 Susceptibility

We performed simulation under conjugated field to calculate the susceptibility $\chi_1 = \frac{\partial \rho}{\partial h}$. We also used the sample variance and the sample mean of the density of infection to calculate the susceptibility χ_2 using Eq. 3.79. The results are depicted in Fig. 4.12 (3-uniform hypergraphs) and Fig. 4.13 (4-uniform hypergraphs). We used 10 values of the field strength h' between 10^{-4} and 10^{-3}, and performed the linear regression

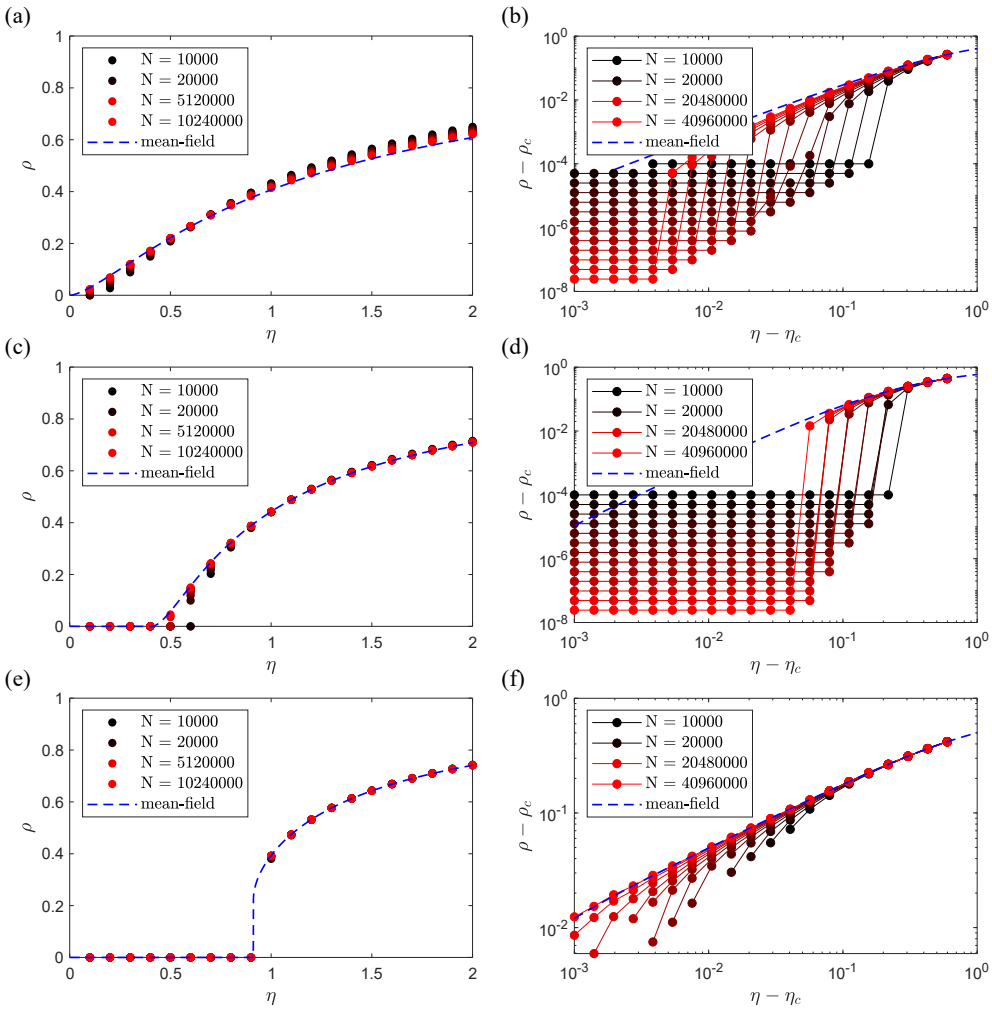

Fig. 4.10: The density of infection of the static model of 3-uniform hypergraphs with degree exponent (a, b) $\lambda = 2.2$, (c, d) $\lambda = 2.5$, and (e, f) $\lambda = 2.8$. The mean degree $\langle k \rangle = d$, which corresponds to $K = 1$ in the static model of uniform hypergraph. Redder dots represent systems with the larger numbers of nodes. The mean-field results are represented by dashed blue lines. As the system size is increased, the numerical results approaches the mean-field results. For $\lambda \leq 2.5$, where the phase transition is expected to be of second-order, the jump of the order parameter at the epidemic threshold approaches zero, while for $\lambda > 2.5$,where the phase transition is predicted to be of first-order, the jump of the order parameter approaches a finite value.

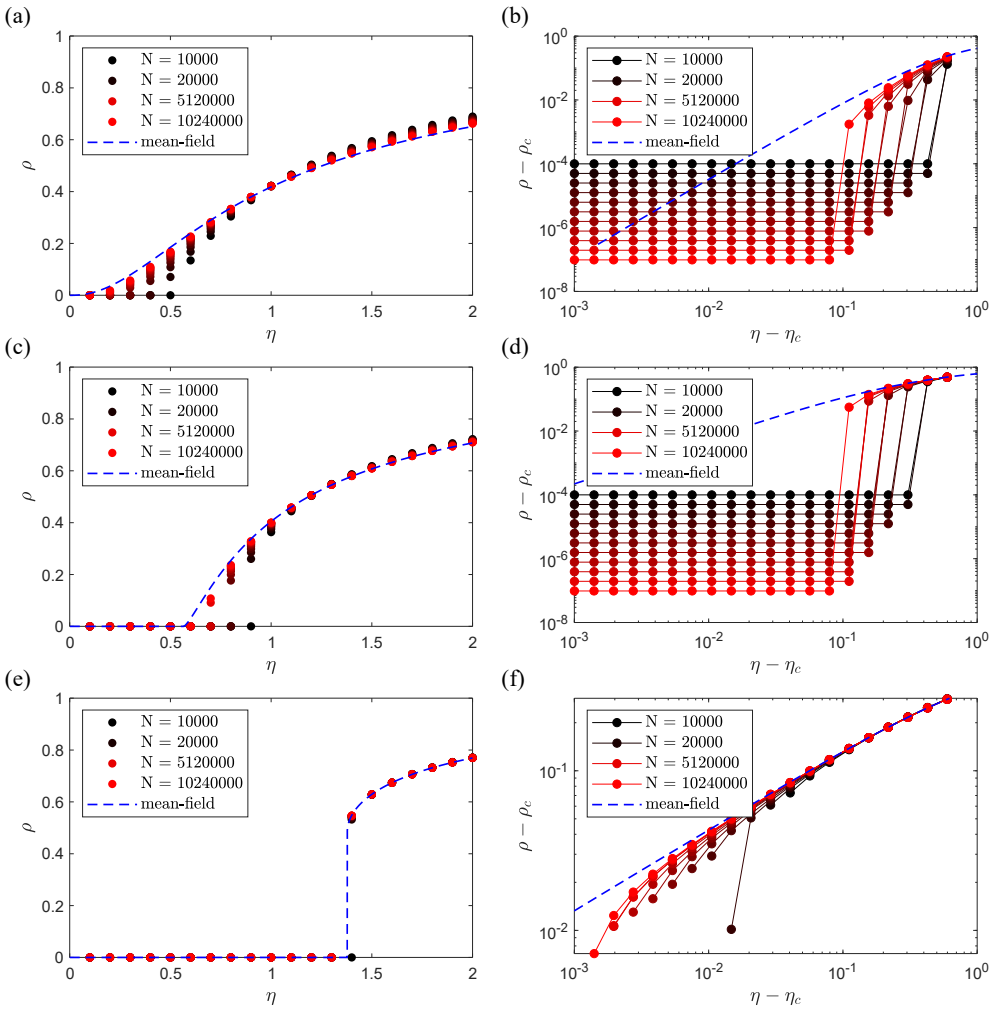

Fig. 4.11: The density of infection of the static model of 4-uniform hypergraphs with degree exponent (a, b) $\lambda = 2.2$, (c, d) $\lambda = 2 + \frac{1}{3}$, and (e, f) $\lambda = 2.8$. The mean degree $\langle k \rangle = d$, which corresponds to $K = 1$ in the static model of uniform hypergraph. Redder dots represent systems with the larger numbers of nodes. The mean-field results are represented by dashed blue lines. As the system size is increased, the numerical results approaches the mean-field results. For $\lambda \leq 2.5$, where the phase transition is expected to be of second-order, the jump of the order parameter at the epidemic threshold approaches zero, while for $\lambda > 2.5$,where the phase transition is predicted to be of first-order, the jump of the order parameter approaches a finite value.

(least-square method) to calculate $\frac{\partial \rho}{\partial h'}$. The susceptibility to the conjugated field χ_1 corroborated the mean-field predictions.

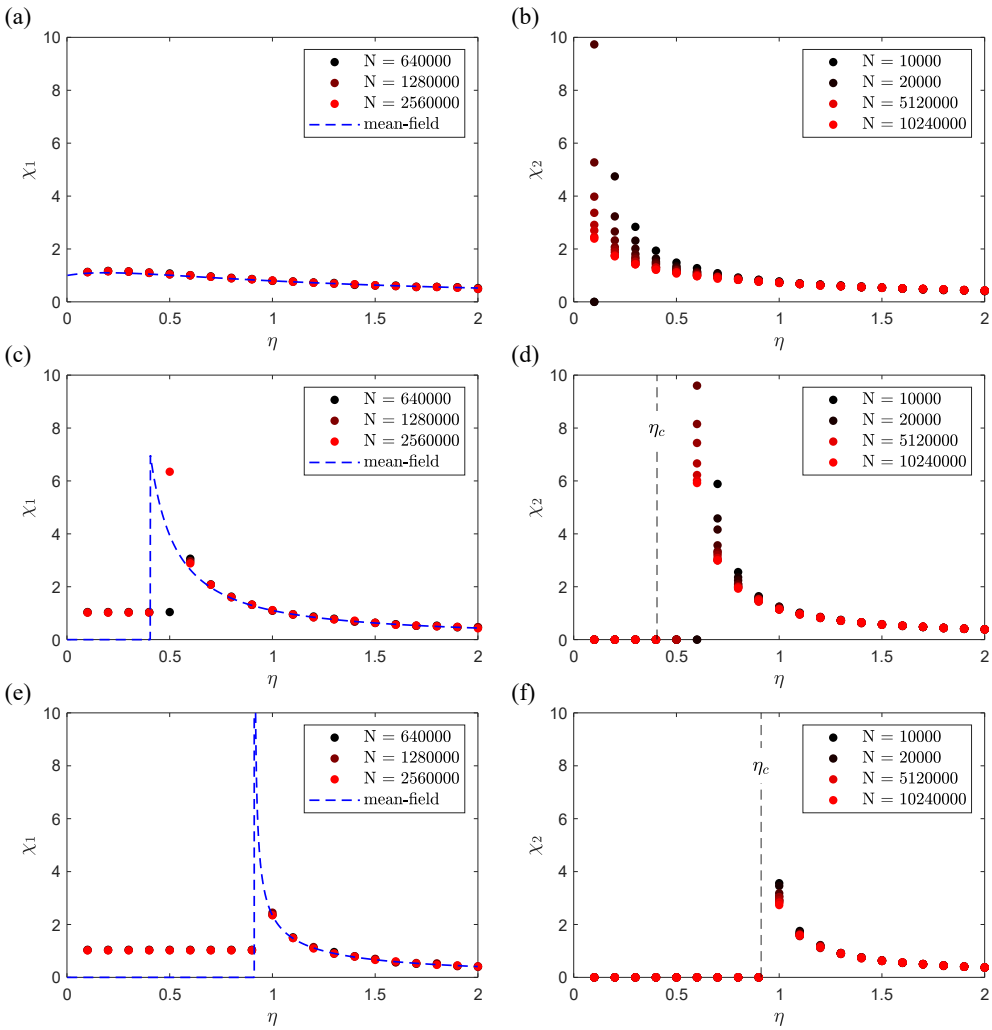

Fig. 4.12: The susceptibility χ_1 of the static model of 3-uniform hypergraphs with the degree exponent (a) $\lambda = 2.2$, (c) $\lambda = 2.5$, and (e) $\lambda = 2.8$, and the susceptibility χ_2 for (b) $\lambda = 2.2$, (d) $\lambda = 2.5$, and (f) $\lambda = 2.8$. The mean degree $\langle k \rangle = d = 3$, which corresponds to $K = 1$ in the static model of uniform hypergraph. The susceptibility χ_1 is calculated by the linear regression of the mean density of infection under small conjugated field $h' = 10^{-4}$–10^{-3} (χ_1). The mean-field results are represented by dashed blue lines.

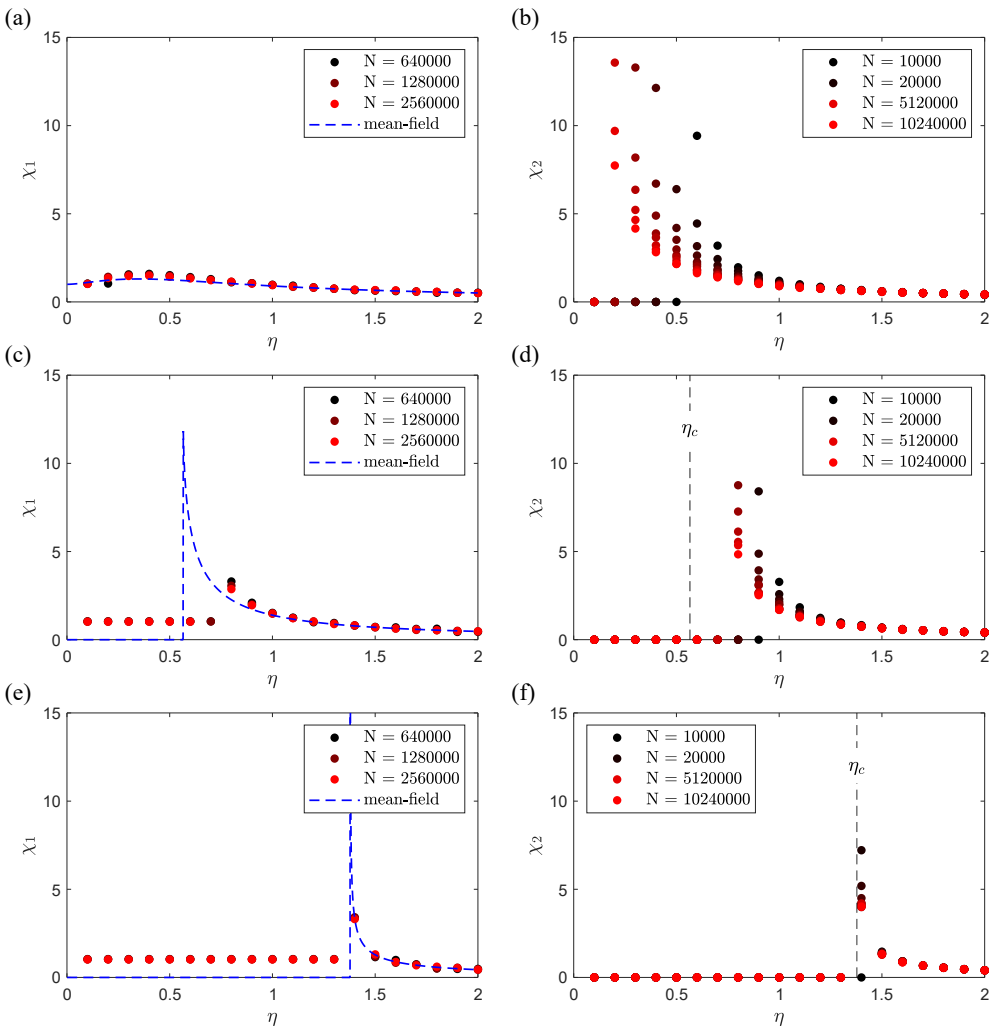

Fig. 4.13: The susceptibility χ_1 of the static model of 4-uniform hypergraphs with the degree exponent (a) $\lambda = 2.2$, (c) $\lambda = 2 + \frac{1}{3}$, and (e) $\lambda = 2.8$, and the susceptibility χ_2 for (b) $\lambda = 2.2$, (d) $\lambda = 2 + \frac{1}{3}$, and (f) $\lambda = 2.8$. The mean degree $\langle k \rangle = d = 4$, which corresponds to $K = 1$ in the static model of uniform hypergraph. The susceptibility χ_1 is calculated by the linear regression of the mean density of infection under small conjugated field $h' = 10^{-4}$–10^{-3} (χ_1). The mean-field results are represented by dashed blue lines.

Chapter 5

Conclusion

In this thesis, we studied the simplicial SIS model in scale-free uniform hypergraph using the static model of uniform hypergraph. We proposed the static model of uniform hypergraph, which is a generalization of the static model of complex network. We showed that the model has a degree distribution with a power-law tail.

We studied the system analytically using the heterogeneous mean-field theory. We found that the system shows a rich phase transition when the exponent of the degree distribution is between two and three. If the degree exponent is below a critical value, which depends on the size of the hyperedges, the epidemic threshold vanishes. Therefore, there is a non-trivial stationary state for arbitrarily small contagion rate. The susceptibility converges to 1 in the vicinity of the epidemic threshold. If the degree exponent is above the critical value, the system shows a first-order phase transition at a finite contagion rate. The susceptibility diverges in the vicinity of the phase transition. If the degree exponent is exactly the critical value, the system undergoes a second-order phase transition at a finite contagion rate. The susceptibility converges to a finite value at the epidemic threshold.

We performed numerical simulations in annealed scale-free 3- and 4-uniform hypergraphs with the degree exponent between 2 and 3. We implemented the quasistationary method to study the properties of the stationary state. The results of the density of infection and the susceptibility corroborated the mean-field theoretical predictions.

Bibliography

[1] D. J. D. S. Price, *Networks of scientific papers*, Science, 510–515 (1965).

[2] A.-L. Barabási and R. Albert, *Emergence of scaling in random networks*, Science **286**, 509–512 (1999).

[3] A.-L. Barabási, *Scale-free networks: a decade and beyond*, Science **325**, 412–413 (2009).

[4] S. Abe and N. Suzuki, *Scale-free network of earthquakes*, EPL **65**, 581 (2004).

[5] H. Ebel, L.-I. Mielsch, and S. Bornholdt, *Scale-free topology of e-mail networks*, Phys. Rev. E **66**, 035103 (2002).

[6] M. Girvan and M. E. Newman, *Community structure in social and biological networks*, Proc. Natl. Acad. Sci. **99**, 7821–7826 (2002).

[7] M. J. Hamilton, B. T. Milne, R. S. Walker, O. Burger, and J. H. Brown, *The complex structure of hunter-gatherer social networks*, Proc. Royal Soc. B **274**, 2195–2203 (2007).

[8] Z. Katona, P. P. Zubcsek, and M. Sarvary, *Network effects and personal influences: The diffusion of an online social network*, J. Mark. Res. **48**, 425–443 (2011).

[9] E. M. Rogers, *A prospective and retrospective look at the diffusion model*, J. Health Commun. **9**, 13–19 (2004).

[10] E. M. Rogers, U. E. Medina, M. A. Rivera, and C. J. Wiley, *Complex adaptive systems and the diffusion of innovations*, Innov. J. Public Sect. Innov. J. **10**, 1–26 (2005).

[11] Y. C. Xu, C. Zhang, L. Xue, and L. L. Yeo, *Product adoption in online social network*, ICIS Proc., 200 (2008).

[12] D. Acemoğlu, G. Como, F. Fagnani, and A. Ozdaglar, *Opinion fluctuations and disagreement in social networks*, Math. Oper. Res. **38**, 1–27 (2013).

[13] A. Grabowski and R. Kosiński, *Ising-based model of opinion formation in a complex network of interpersonal interactions*, Physica A: Statistical Mechanics and its Applications **361**, 651–664 (2006).

[14] D. J. Watts and P. S. Dodds, *Influentials, networks, and public opinion formation*, J. Consumer Res. **34**, 441–458 (2007).

[15] S. P. Borgatti and P. C. Foster, *The network paradigm in organizational research: A review and typology*, J. Manag. **29**, 991–1013 (2003).

[16] S. Boccaletti, V. Latora, Y. Moreno, M. Chavez, and D.-U. Hwang, *Complex networks: Structure and dynamics*, Phys. Rep. **424**, 175–308 (2006).

[17] H. Hoang and B. Antoncic, *Network-based research in entrepreneurship: A critical review*, J. Bus. Ventur. **18**, 165–187 (2003).

[18] M. E. Newman, *The structure and function of complex networks*, SIAM Rev. **45**, 167–256 (2003).

[19] K. G. Provan, A. Fish, and J. Sydow, *Interorganizational networks at the network level: A review of the empirical literature on whole networks*, J. Manag. **33**, 479–516 (2007).

[20] R. Pastor-Satorras and A. Vespignani, *Epidemic dynamics and endemic states in complex networks*, Phys. Rev. E **63**, 066117 (2001).

[21] R. Pastor-Satorras and A. Vespignani, *Epidemic spreading in scale-free networks*, Phys. Rev. Lett. **86**, 3200 (2001).

[22] M. Boguná and R. Pastor-Satorras, *Epidemic spreading in correlated complex networks*, Phys. Rev. E **66**, 047104 (2002).

[23] Y. Moreno, R. Pastor-Satorras, and A. Vespignani, *Epidemic outbreaks in complex heterogeneous networks*, Eur. Phys. J. B **26**, 521–529 (2002).

[24] H.-K. Janssen, M. Müller, and O. Stenull, *Generalized epidemic process and tricritical dynamic percolation*, Phys. Rev. E **70**, 026114 (2004).

[25] R. Pastor-Satorras, C. Castellano, P. Van Mieghem, and A. Vespignani, *Epidemic processes in complex networks*, Rev. Mod. Phys. **87**, 925 (2015).

[26] C. Castellano and R. Pastor-Satorras, *Thresholds for epidemic spreading in networks*, Phys. Rev. Lett. **105**, 218701 (2010).

[27] H. K. Lee, P.-S. Shim, and J. D. Noh, *Epidemic threshold of the susceptible-infected-susceptible model on complex networks*, Phys. Rev. E **87**, 062812 (2013).

[28] W. Choi, D. Lee, and B. Kahng, *Mixed-order phase transition in a two-step contagion model with a single infectious seed*, Phys. Rev. E **95**, 022304 (2017).

[29] W. Choi, D. Lee, and B. Kahng, *Critical behavior of a two-step contagion model with multiple seeds*, Phys. Rev. E **95**, 062115 (2017).

[30] M. Karsai, G. Iniguez, K. Kaski, and J. Kertész, *Complex contagion process in spreading of online innovation*, J. Royal Soc. Interface **11**, 20140694 (2014).

[31] D. Centola and M. Macy, *Complex contagions and the weakness of long ties*, Am. J. Sociol. **113**, 702–734 (2007).

[32] I. Iacopini, G. Petri, A. Barrat, and V. Latora, *Simplicial models of social contagion*, Nat. Commun. **10**, 2485 (2019).

[33] G. Ghoshal, V. Zlatić, G. Caldarelli, and M. E. Newman, *Random hypergraphs and their applications*, Phys. Rev. E **79**, 066118 (2009).

[34] D. Bollé, R. Heylen, and N. Skantzos, *Thermodynamics of spin systems on small-world hypergraphs*, Phys. Rev. E **74**, 056111 (2006).

[35] D. Bollé and R. Heylen, *Small-world hypergraphs on a bond-disordered bethe lattice*, Phys. Rev. E **77**, 046104 (2008).

[36] S. Klamt, U.-U. Haus, and F. Theis, *Hypergraphs and cellular networks*, PLOS Comput. Biol. **5**, e1000385 (2009).

[37] C. Taramasco, J.-P. Cointet, and C. Roth, *Academic team formation as evolving hypergraphs*, Scientometrics **85**, 721–740 (2010).

[38] A. Vazquez, *Population stratification using a statistical model on hypergraphs*, Phys. Rev. E **77**, 066106 (2008).

[39] Z.-K. Zhang and C. Liu, *A hypergraph model of social tagging networks*, J. Stat. Mech.: Theory Exp. **2010**, P10005 (2010).

[40] V. Zlatić, G. Ghoshal, and G. Caldarelli, *Hypergraph topological quantities for tagged social networks*, Phys. Rev. E **80**, 036118 (2009).

[41] g. Bodó, G. Y. Katona, and P. L. Simon, *Sis epidemic propagation on hypergraphs*, Bull. Math. Biol. **78**, 713–735 (2016).

[42] Q. Suo, J.-L. Guo, and A.-Z. Shen, *Information spreading dynamics in hypernetworks*, Physica A **495**, 475–487 (2018).

[43] Z. Xie, Z. Ouyang, and J. Li, *A geometric graph model for coauthorship networks*, Journal of Informetrics **10**, 299–311 (2016).

[44] E. N. Ciftcioglu, R. Ramanathan, and P. Basu, *Generative models for global collaboration relationships*, Sci. Rep. **7**, 11160 (2017).

[45] A. Patania, G. Petri, and F. Vaccarino, *The shape of collaborations*, Eur. Phys. J. DS **6**, 18 (2017).

[46] A. E. Sizemore, E. A. Karuza, C. Giusti, and D. S. Bassett, *Knowledge gaps in the early growth of semantic networks*, arXiv:1709.00133, journal (2017).

[47] E. Estrada and G. J. Ross, *Centralities in simplicial complexes. applications to protein interaction networks*, J. Theor. Biol. **438**, 46–60 (2018).

[48] H. Lee, H. Kang, M. K. Chung, B.-N. Kim, and D. S. Lee, *Persistent brain network homology from the perspective of dendrogram*, IEEE Trans. Med. Imaging **31**, 2267–2277 (2012).

[49] G. Petri, P. Expert, F. Turkheimer, R. Carhart-Harris, D. Nutt, P. J. Hellyer, and F. Vaccarino, *Homological scaffolds of brain functional networks*, J. Royal Soc. Interface **11**, 20140873 (2014).

[50] G. Bianconi and C. Rahmede, *Complex quantum network manifolds in dimension d >2 are scale-free*, Sci. Rep. **5**, 13979 (2015).

[51] G. Bianconi and C. Rahmede, *Network geometry with flavor: from complexity to quantum geometry*, Phys. Rev. E **93**, 032315 (2016).

[52] O. T. Courtney and G. Bianconi, *Generalized network structures: The configuration model and the canonical ensemble of simplicial complexes*, Phys. Rev. E **93**, 062311 (2016).

[53] O. T. Courtney and G. Bianconi, *Weighted growing simplicial complexes*, Phys. Rev. E **95**, 062301 (2017).

[54] G. Petri and A. Barrat, *Simplicial activity driven model*, Phys. Rev. Lett. **121**, 228301 (2018).

[55] C. I. Del Genio, H. Kim, Z. Toroczkai, and K. E. Bassler, *Efficient and exact sampling of simple graphs with given arbitrary degree sequence*, PLOS ONE **5**, e10012 (2010).

[56] P. Erdős and T. Gallai, *Graphs with prescribed degrees of vertices*, Mat. Lapok **11**, 264–274 (1960).

[57] J.-G. Young, G. Petri, F. Vaccarino, and A. Patania, *Construction of and efficient sampling from the simplicial configuration model*, Phys. Rev. E **96**, 032312 (2017).

[58] K.-I. Goh, B. Kahng, and D. Kim, *Universal behavior of load distribution in scale-free networks*, Phys. Rev. Lett. **87**, 278701 (2001).

[59] J.-S. Lee, K.-I. Goh, B. Kahng, and D. Kim, *Intrinsic degree-correlations in the static model of scale-free networks*, Eur. Phys. J. B **49**, 231–238 (2006).

[60] D.-S. Lee, K.-I. Goh, B. Kahng, and D. Kim, *Scale-free random graphs and potts model*, Pramana **64**, 1149–1159 (2005).

[61] K.-I. Goh, D.-S. Lee, B. Kahng, and D. Kim, *Sandpile on scale-free networks*, Phys. Rev. Lett. **91**, 148701 (2003).

[62] D.-H. Kim, G. Rodgers, B. Kahng, and D. Kim, *Spin-glass phase transition on scale-free networks*, Phys. Rev. E **71**, 056115 (2005).

[63] C.-M. Ghim, E. Oh, K.-I. Goh, B. Kahng, and D. Kim, *Packet transport along the shortest pathways in scale-free networks*, Eur. Phys. J. B **38**, 193–199 (2004).

[64] S. H. Lee, H. Jeong, and J. D. Noh, *Random field ising model on networks with inhomogeneous connections*, Phys. Rev. E **74**, 031118 (2006).

[65] J.-S. Yang, W. Kwak, K.-I. Goh, and I.-m. Kim, *Critical behavior of the xy model on static scale-free networks*, EPL **84**, 36004 (2008).

[66] H. Yi, *Quantum fluctuations in a scale-free network-connected ising system*, Eur. Phys. J. B **61**, 89–93 (2008).

[67] E. O. Nsoesie, J. S. Brownstein, N. Ramakrishnan, and M. V. Marathe, *A systematic review of studies on forecasting the dynamics of influenza outbreaks*, Influenze Other Resp. **8**, 309–316 (2014).

[68] M. Tizzoni, P. Bajardi, C. Poletto, J. J. Ramasco, D. Balcan, B. Gonçalves, N. Perra, V. Colizza, and A. Vespignani, *Real-time numerical forecast of global epidemic spreading: case study of 2009 a/h1n1pdm*, BMC Med. **10**, 165 (2012).

[69] T. W. Valente, *Network models of the diffusion of innovations*, Comput. Math. Organ. Theory **2**, 163–164 (1996).

[70] C. Heath, C. Bell, and E. Sternberg, *Emotional selection in memes: the case of urban legends*, J. Pers. Soc. Psychol. **81**, 1028 (2001).

[71] J. S. Coleman, E. Katz, and H. Menzel, *Medical innovation: A diffusion study*, Bobbs-Merrill Co (1966).

[72] J. S. MacDonald and L. D. MacDonald, *Chain migration ethnic neighborhood formation and social networks*, Milbank Q. **42**, 82–97 (1964).

[73] D. Crane, *Diffusion models and fashion: a reassessment*, The Annals of the American Academy of Political and Social Science **566**, 13–24 (1999).

[74] M. Granovetter, *Threshold models of collective behavior*, Am. J. Sociol. **83**, 1420–1443 (1978).

[75] D. J. Watts, *A simple model of global cascades on random networks*, Proc. Natl. Acad. Sci. **99**, 5766–5771 (2002).

[76] J. Chalupa, P. L. Leath, and G. R. Reich, *Bootstrap percolation on a bethe lattice*, J. Phys. Condens. Matter **12**, L31 (1979).

[77] P. Comon, G. Golub, L.-H. Lim, and B. Mourrain, *Symmetric tensors and symmetric tensor rank*, SIAM J. Matrix Anal. Appl. **30**, 1254–1279 (2008).

[78] M. Abramowitz and I. A. Stegun, *Handbook of mathematical functions: with formulas, graphs, and mathematical tables*, Courier Corporation (1965).

[79] S. Lübeck, *Tricritical directed percolation*, J. Stat. Phys. **123**, 193–221 (2006).

[80] H. Hinrichsen, *Non-equilibrium critical phenomena and phase transitions into absorbing states*, Adv. Phys. **49**, 815–958 (2000).

[81] P. Grassberger, *Tricritical directed percolation in 2+ 1 dimensions*, J. Stat. Mech.: Theory Exp. **2006**, P01004 (2006).

[82] S. C. Ferreira, C. Castellano, and R. Pastor-Satorras, *Epidemic thresholds of the susceptible-infected-susceptible model on networks: A comparison of numerical and theoretical results*, Phys. Rev. E **86**, 041125 (2012).

[83] C. Castellano and R. Pastor-Satorras, *Routes to thermodynamic limit on scale-free networks*, Phys. Rev. Lett. **100**, 148701 (2008).

[84] P. G. Fennell, S. Melnik, and J. P. Gleeson, *Limitations of discrete-time approaches to continuous-time contagion dynamics*, Phys. Rev. E **94**, 052125 (2016).

[85] A. J. Walker, *An efficient method for generating discrete random variables with general distributions*, ACM Trans. Math. Softw. **3**, 253–256 (1977).

[86] J. Marro and R. Dickman, *Nonequilibrium phase transitions in lattice models*, Cambridge University Press (2005).

[87] S. C. Ferreira, R. S. Ferreira, and R. Pastor-Satorras, *Quasistationary analysis of the contact process on annealed scale-free networks*, Phys. Rev. E **83**, 066113 (2011).

[88] E. Volz and L. A. Meyers, *Epidemic thresholds in dynamic contact networks*, J. Royal Soc. Interface **6**, 233–241 (2008).

[89] S. H. Lee, M. Ha, H. Jeong, J. D. Noh, and H. Park, *Critical behavior of the ising model in annealed scale-free networks*, Phys. Rev. E **80**, 051127 (2009).

[90] C. W. Gardiner et al., *Handbook of stochastic methods*, Springer Berlin (1985).

초 록

하이퍼그래프는 그래프보다 더 복잡하고 많은 요소들이 동시에 상호작용하는 현상을 기술할 수 있다. 최근에 하이퍼그래프에서 complex contagion process로써 simplicial contagion process가 제안되었다. Simplicial contagion process를 통해 감염이 전파되는 SIS 모형을 simplicial SIS 모형이라 부른다. 이 학위논문에서는 simplicial SIS 모형을 척도 없는 균일 하이퍼그래프에서 연구하였다. 평균장 이론을 사용하여 이 모형에서 상전이의 성질을 연구하였고, 시뮬레이션으로 그 예측을 검증하였다. 이 모델이 도수 분포함수의 지수가 2와 3 사이일 때 다양한 상전이 현상을 보인다는 것을 발견하였다. 상전이의 성질들이 도수 분포함수의 지수에 따라 완전히 달라진다. 지수가 어떤 임계값보다 작을 경우에는 전염현상의 문턱값이 0이 되고, 상전이 점 근처에서 감수율이 0이 아닌 유한한 값으로 수렴한다. 지수가 임계값과 정확히 같을 경우에는 0이 아닌 유한한 문턱값에서 2차 상전이가 일어나게 되며, 감수율은 0이 아닌 유한한 값으로 수렴한다. 지수가 임계값보다 클 경우에는 0이 아닌 유한한 문턱값에서 1차 상전이가 일어나게 되며, 감수율은 무한대로 발산한다. 도수 분포함수의 지수의 임계값은 하이퍼그래프 내의 하이퍼엣지의 크기의 함수로 주어지며 2와 3 사이의 값을 가진다. 시뮬레이션 결과는 평균장 이론으로 계산한 예측값과 일치하였다.

주요어 : 전염병 확산 과정, SIS 모형, 척도 없는 네트워크, 균일 하이퍼그래프, 척도 없는 하이퍼그래프, 상전이

학번 : 2017-24896